Developmental Biology 344 (2010) 36–51

Contents lists available at ScienceDirect

Developmental Biology

journal homepage: www.elsevier.com/developmentalbiology

Geminin and Brahma act antagonistically to regulate EGFR–Ras–MAPK signaling in *Drosophila*

Anabel Herr [a,b,1], Lisa Mckenzie [a,1], Randy Suryadinata [c], Martin Sadowski [c], Linda M. Parsons [a], Boris Sarcevic [c,d], Helena E. Richardson [a,b,e,*]

[a] Peter MacCallum Cancer Center, Melbourne, Victoria, Australia
[b] Anatomy and Cell Biology Department, University of Melbourne, Melbourne, Victoria, Australia
[c] St Vincent's Institute, Melbourne, Victoria, Australia
[d] Department of Medicine, University of Melbourne, Melbourne, Victoria, Australia
[e] Department of Biochemistry and Molecular Biology, University of Melbourne, Melbourne, Victoria, Australia

ARTICLE INFO

Article history:
Received for publication 19 February 2010
Revised 4 April 2010
Accepted 8 April 2010
Available online 21 April 2010

Keywords:
Drosophila
Brahma complex
Geminin
EGFR signalling
Wing development

ABSTRACT

Geminin was identified in *Xenopus* as a dual function protein involved in the regulation of DNA replication and neural differentiation. In *Xenopus*, Geminin acts to antagonize the Brahma (Brm) chromatin-remodeling protein, Brg1, during neural differentiation. Here, we investigate the interaction of Geminin with the Brm complex during *Drosophila* development. We demonstrate that *Drosophila* Geminin (Gem) interacts antagonistically with the Brm–BAP complex during wing development. Moreover, we show *in vivo* during wing development and biochemically that Brm acts to promote EGFR–Ras–MAPK signaling, as indicated by its effects on pERK levels, while Gem opposes this. Furthermore, *gem* and *brm* alleles modulate the wing phenotype of a Raf gain-of-function mutant and the eye phenotype of a EGFR gain-of-function mutant. Western analysis revealed that Gem over-expression in a background compromised for Brm function reduces Mek (MAPKK/Sor) protein levels, consistent with the decrease in ERK activation observed. Taken together, our results show that Gem and Brm act antagonistically to modulate the EGFR–Ras–MAPK signaling pathway, by affecting Mek levels during *Drosophila* development.

Introduction

During development coordination between cell proliferation and terminal differentiation is critical to enable cells to cease division and differentiate appropriately. In order to achieve this, tight regulation of the cell cycle occurs, predominantly at the G1 to S-phase transition, to allow the appropriate response to external signals (Hunter and Pines, 1994). The G1- to S-phase transition is driven by the regulated activity of G1 Cyclin/Cyclin-dependent kinase (Cdk) complexes, Cyclin D/Cdk4(6) and Cyclin E/Cdk2 (Reed, 1997). These kinases drive the G1 to S-phase progression by phosphorylating key substrates that are required for S-phase gene transcription and for the initiation of DNA replication. To ensure that DNA is replicated only once per cell cycle the initiation of DNA replication requires periodic activation and inactivation of G1 Cyclin/CDKs, as assembly of the pre-replication complex (pre-RC) at replication origins can only occur during low Cdk activity period (late mitosis to G1) (Bell and Dutta, 2002; Diffley, 2004; Fujita, 1999). Assembly of the pre-RC or "licensing reaction" involves loading the Mini-Chromosome-Maintenance (MCM) protein complex onto chromatin by the origin recognition complex (ORC) and two essential factors, CDC6 and Cdt1 (Maiorano et al., 2000; Nishitani et al., 2000). In yeast, the periodic activation and inactivation of Cdk activity is sufficient to enable licensing, however in more complex eukaryotes, an additional control mechanism has been discovered. In *Drosophila*, *Xenopus* and mammals, Geminin binds Cdt1, preventing the loading of the MCMs onto the chromatin and thereby suppressing inappropriate re-assembly of the pre-RC during S-, G2- and M-phase (Lygerou and Nurse, 2000; McGarry and Kirschner, 1998; Wohlschlegel et al., 2000).

Geminin is a bi-functional protein in *Xenopus*, whose C-terminal cell cycle domain can inhibit DNA replication and whose N-terminal neuralization domain has an essential role in specifying neural cell fate (Kroll et al., 1998; McGarry and Kirschner, 1998). In *Drosophila*, Geminin (Gem) is expressed in dividing cells, including the neuroblasts of the peripheral (PNS) and central nervous systems (CNS), and is down-regulated when cells stop dividing and commence differentiation (Quinn et al., 2001). Our previous studies showed that *gem* mutant embryos over-replicate DNA exhibiting anaphase defects, as well as a loss of the dorsal-most peripheral neurons in late stage embryos (Quinn et al., 2001). Conversely, ectopic expression of *Drosophila* Gem inhibits DNA replication and cells enter mitosis with

* Corresponding author: Peter MacCallum Cancer Center, St Andrews Place, East Melbourne, 3002, Victoria, Australia.
E-mail address: Helena.richardson@petermac.org (H.E. Richardson).
[1] These authors contributed equally to the manuscript.

0012-1606/$ – see front matter
doi:10.1016/j.ydbio.2010.04.006

under-replicated DNA and undergo apoptosis. We also showed that over-expression of Gem leads to ectopic neural cells in the embryonic epidermis. However, from these studies it was unclear whether these ectopic neural cells are a result of cell cycle defects or reflect a more specific role for Gem in neural differentiation.

Xenopus Geminin was shown to functionally interact with the catalytic subunit of the SWI/SNF chromatin-remodeling complex, resulting in changes in transcription (Seo et al., 2005). This study also showed that Geminin controls the transition from proliferating precursors to differentiated post-mitotic neurons by modulating interactions between SWI/SNF and bHLH transcription factors that are critical for neurogenesis (Seo et al., 2005). In other developmental contexts, for example during eye development in the fish, Medaka, and during neural tube development in the chicken, Geminin mediates proliferative-differentiation transitions through interactions with the transcription factors Six3 and Hox, as well as Polycomb Group proteins (Del Bene et al., 2004; Luo et al., 2004). Interactions between Geminin and transcription factors, or the Polycomb or SWI/SNF chromatin-remodeling complex proteins reveal a novel role for Geminin in transcriptional control. In the yeast, *Saccharomyces cerevisiae*, the SWI/SNF protein complex functions through ATP-dependent chromatin remodeling to control gene expression at specific promoters (Kingston et al., 1996). Mammalian homologs of the Swi2 ATPase subunit, Brahma (Brm) and Brg1, induce cell cycle arrest when ectopically expressed (Bultman et al., 2000; Muchardt and Yaniv, 2001). Furthermore, Brm knockout mice show hyperplasia of organs (Reyes et al., 1998), while Brg1 knockouts are early embryonic lethal, but heterozygous mice are predisposed to tumor formation (Bultman et al., 2000). Taken together these studies demonstrate interactions between Geminin and transcription factors, the Polycomb complex or the SWI/SNF (Brm or Brg1) chromatin-remodeling complex, and reveal roles for Geminin in the transcriptional control of cell cycle exit and differentiation.

In *Drosophila* the SWI/SNF homologue *brahma* (*brm*) is an essential gene (Elfring et al., 1998). *brm* mutants show a decrease in viability and defects in the peripheral nervous system (PNS) of adults. Furthermore, a dominant-negative form of *brahma*, brm^{K0804R}, (brm^{DN}) which is defective for ATP hydrolysis but shows normal complex assembly (Elfring et al., 1998), displays defects in the PNS and homeotic transformations. Genome-wide analysis of the Brm complex in larval salivary glands, has shown that the Brm complex is associated with nearly all transcriptionally active sites and reduction of Brm function dramatically reduces the association of RNA polymerase II with salivary gland chromosomes (Armstrong et al., 2002). Analysis of the *Drosophila* Brm complex revealed two different complexes, BAP (defined by the presence of the SWI1 homolog, Osa), and PBAP (defined by Polybromo and BAP170) that bind to different regions on polytene chromosomes (Collins et al., 1999; Moshkin et al., 2007). Furthermore, Affymetrics microarray analysis of RNAi knockdown of each complex in S2 cells showed that they direct distinct transcriptional programs (Mohrmann et al., 2004; Moshkin et al., 2007). However, what the critical targets of these Brm complexes are in specific tissues and how these targets may be modulated during development is unclear. An insight into this key issue has come from a genetic screen for modifiers of the *brahma* dominant-negative mutant phenotype (Armstrong et al., 2005). This study revealed mutations in genes involved in the Notch and EGF receptor (EGFR)–Ras–MAPK signaling pathway (Armstrong et al., 2005), suggesting that these signaling pathways may be targets of Brm or act to modulate the activity of the Brm complex. Moreover in wing vein development, the Brm complex was shown to modulate expression of genes in the EGFR–Ras–MAPK and Decapentapelgic (Dpp/TGFβ) signaling pathways (Marenda et al., 2004).

In this study, we investigate the interaction between Gem and the Brm complex in *Drosophila*. We show that Gem and Brm form a complex and genetically interact in an antagonistic manner. We also demonstrate that *Drosophila* Gem interacts antagonistically with other members of the Brm–BAP complex during wing development. Moreover, we provide genetic and biochemical evidence that Brm promotes, while Gem inhibits, EGFR–Ras–MAPK signalling during development.

Materials and methods

Fly strains used and genetic analysis

The *UAS-*brm^{K804R} (brm^{DN}) transgenic flies carry a dominant-negative form of *brahma*, which contains a mutation in the ATP-binding site of the Brm protein that eliminates Brm function *in vivo*, but does not affect assembly of the 2-MD Brm complex (Elfring et al., 1998). Gem was ectopically expressed using a weaker *UAS-gem* transgene, *UAS-*gem^{43} (Quinn et al., 2001). Other fly stocks used were: *UAS-Snr1* and *UAS-Snr1-cdel.3* ($Snr1^{DN}$) (Zraly et al., 2003), *UAS-Osa* (Collins et al., 1999) and *en-GAL4*, *UAS-GFP* and *C96-GAL4* were provided by Laura Johnston. All other fly strains were obtained from Bloomington Stock Center (Bloomington, Indiana) or generated in the laboratory. For all experiments flies were raised on standard cornmeal agar food at 25 °C unless otherwise indicated.

UAS-gem dsRNA transgenic flies were generated by amplifying a 500 bp fragment from the *gem* coding region using specific PCR primers (shown below) and ligated as inverted repeats in the *pWIZ* plasmid using the AvrII and NheI sites (Lee and Carthew, 2003), and verified by DNA sequencing. The *UAS-gem-dsRNA* line M4 (3rd chromosome), which resulted in the stronger knockdown of Gem compared with a second line, M6 (data not shown), was used in this study.

UAS-brm^{WT} transgenic flies were derived from a construct in *pUAST* (Brand et al., 1994) containing the full-length Brm cDNA. The Brm cDNA from pOT2-Brm (clone LD36356, Berkeley *Drosophila* Genome Project) was amplified by PCR using the primers shown below and ligated into *pUAST* using the restriction enzymes NotI and XbaI, and verified by DNA sequencing.

UAS-Raf^{GOF} contains an N-terminal deletion of the Raf (Phl) coding sequence from amino acids 2 to 431 and generates a constitutively activated version of Raf, under the control of the *S. cerevisiae UAS* enhancer (Brand et al., 1994; Brand and Perrimon, 1994). To examine genetic interaction with Brm or Gem and Raf^{GOF}, recombinant flies were generated containing the *C96-GAL4* (chromosome 3) with *UAS-*Raf^{GOF} (chromosome 3) and these flies were crossed either to *UAS-GFP* or to *UAS-gem* or *UAS-*brm^{DN} or double transgenic flies.

For genetic interactions of adult eyes or wing phenotypes, at least 50 progeny were scored for each cross and representative images for each genotype are shown. For analysis of adult wings, progeny were fixed in xylene and wings were dissected and mounted in Canadian Balsam and photographed on an Olympus BX-51 microscope at 4× magnification.

Primer sequences

Gem dsRNA

Forward: 5′GATGTCTAGAAGCGCTGCCAGGGTCTA 3′
Reverse: 5′ TCCTTCTAGACGCTGTTGTCCTCTTCGC 3′

Brm full-length cDNA

BrmWT-NotI-SacI: 5′ATAAGAATGCGGCCGCGAGCTCATGGCCTCGCCCTC TCCG 3′

BrmWT-XbaI: 5′ GCGGTCGACTCTAGAGAGCTCCTAGTCCATGTCATCGTCG 3′

Antibody staining for immunofluorescence

All antibody stainings were carried out in 5% goat serum, PBS, 0.1% Triton X-100.

Primary antibodies: rabbit anti-phospho-Histone H3 (PH3 1:400, Upstate Cell Signaling Solutions), mouse anti-phospho-ERK (pERK 1:250, Sigma), mouse anti-Cut and anti-22C10 (1:5, Developmental Hybridoma Bank), rabbit anti-GFP (1:1000, Molecular Probes/Invitrogen). Secondary antibodies: anti-rabbit/mouse/rat Alexa 488, anti-rabbit/mouse/rat Cy3 and anti-rabbit/mouse/rat Cy5 were used 1:500 (Jackson Immunoresearch).

BrdU labeling

Wing discs from 3rd instar larvae were labeled in Schneider media with 0.2 mg/ml BrdU (Sigma) at room temperature for 30 min. Wing discs were fixed for 30 min at 4 °C in 4% formaldehyde PBS, 0.1% Triton X-100 and BrdU was detected with a mouse anti-BrdU antibody (Becton Dickinson, 1:50 in 5% goat serum/PBS, 0.1% Triton X-100). Cy3 donkey anti-mouse (Jackson Immunolaboratories, 1:500 in 5% goat serum/PBS, 0.1% Triton X-100) was used as a secondary antibody.

TUNEL assays

Apoptotic cells were detected by TUNEL staining using the *in situ* cell death detection kit, TMR Red (Roche).

Microscopy

Bright field microscopy was carried out on a Zeiss Axioplan 2 with Nomarski optics. Images were captured with the SPOT advanced CCD cooled digital camera. Fluorescence microscopy was carried out using the Zeiss Axioplan 2 with epi-fluorescence and images captured as above, or using the Bio-rad MRC-1000 confocal on a Leica DMRBE microscope excited by a 488 nm excitation line and a 522DF32 emission filter (green), a 568 nm excitation line and a 605DF32 emission filter (red), or a 647 nm excitation line and a 680DF32 emission filter (far red). Images were captured with the LaserSharp 2000 computer program. Adobe Photoshop and Adobe Illustrator were used to generate the Figures in this paper.

Culturing of S2 cells and expression of Brm^{WT}

D. melanogaster S2 cells stably transfected with pMT/V5-His vector or pMT/V5-His-FLAG tagged Brahma were cultured in Schneider's insect medium (Sigma) containing 10% heat-inactivated foetal calf serum and 200 µg/ml hygromycin B at 27 °C. Brahma protein expression was induced by the addition of 250 µM Cu^{2+}. Cells were collected by centrifugation, washed in PBS twice and lysed in lysis buffer (50 mM Hepes, Ph 7.5, 150 mM NaCl, 1% Triton X-100, 0.5 mM DTT, 10 µg/ml aprotinin, 10 µg/ml leupeptin and 1 mM PMSF), prior to SDS-PAGE and Western blotting.

Western analysis and immunoprecipitation analysis

Third instar larvae were heat-shocked for 1 h, and then allowed to recover for either 1 h or 2 h before the protein lysates from either heads or wing discs were prepared. Co-immunoprecipitation was carried out as previously described (Brumby et al., 2002). Briefly, protein lysates from third instar larval heads were homogenized in NTEN buffer with 1 mM PMSF protease inhibitor. For the Brm immunoprecipitation 330 µg of protein was used and 30 µg of protein was run for a Western, to determine the input level, whereas for the Snr1 immunoprecipitation 220 µg of protein was used and 20 µg of protein was run for a Western. The lysates were then incubated with various antibodies or rabbit pre-immune sera bound to protein G sephasose beads (GE healthcare). Beads were blocked in 5% goat serum in NTEN buffer 3 times for 1 h total and then washed in NTEN buffer 3 times for 1 h total and a 50/50 slurry was made with the beads and NTEN buffer. 30 µl of the bead slurry was then bound to the protein and run on SDS-PAGE gel and immunoblotted.

Primary antibodies used were: polyclonal rat anti-Gem antibody (1:1000) (Quinn et al., 2001), polyclonal rabbit anti-Brm antibody (1:1000, from C. Muchardt), polyclonal rabbit anti-Snr1 (1:1000, from C. Muchardt), monoclonal mouse anti-alpha tubulin (1:10,000, Cell Biochem), monoclonal mouse anti-pERK (diphosphorylated ERK1/2/MAPK1/2, 1:10,000, #M8159 Sigma), rabbit anti-pMEK (pMEK1/2-$S^{217/221}$, 1:10,000, #9154 Cell Signalling), rabbit anti-ERK (MAPK, 1:10,000, #4695 Cell Signalling) and rabbit anti-MEK (MEK1/2, 1:10,000, #9122 Cell Signalling), anti-FLAG (1:1000, M2, Sigma, F1804). Secondary antibodies used were: anti-mouse HRP (1:5000, Jackson Immun), anti-rat HRP (1:5000, Jackson Immun), anti-rabbit HRP (1:5000, Jackson Immun).

Statistical analysis of adult wing phenotypes

Images of adult wings were analyzed using the MetaMorph program. The total area of wing tissue was found by drawing a line around the edge of the wing and calculating the total area within. The area of wing tissue missing was found by calculating the estimated area of wing tissue missing per notch using the same method as above, then adding this together. The total area of wing expected in a wild-type context was calculated by adding the total area of wing tissue with the area of wing tissue missing. The percentage of wing tissue missing was calculated by comparing the total area of wing expected in a wild-type context with the area of wing tissue missing. The percentage of wing area missing was compared between genotypes using a One-way ANOVA and Tukey test using the Graphpad prism program version 5.01. Subsequent graphs were also created using the Graphpad prism program version 5.01.

Statistical analysis for quantification of BrdU, PH3 and TUNEL labeled cells

In order to quantify the amount of BrdU incorporation, PH3 staining the pixel intensity in a set area was determined for a minimum of 10 wing discs per genotype. To quantify TUNEL incorporation, the number of cells that stained for TUNEL in a set area of the wing disc was counted, using a minimum of 10 wing discs per genotype. The average number of cells in a given area was compared between genotypes using a One-way ANOVA and Tukey test using the Graphpad prism version 5.01. Subsequent graphs were also created using the Graphpad prism version 5.01.

Method for quantification of Western bands for graphs

The Western bands intensity was measured using the ImageJ program, and then normalized to the intensity value of the α-tubulin control. These values were then expressed as a fold difference compared with the wild-type control. Calculations were made using Microsoft Excel. Graphs were made using GraphPad Prism version 5.01.

To determine the stoichiometry of interactions between Gem, Brm and Snr1, we measured the relative amount of Gem protein to Brm or Snr1 protein in the immunoprecipitations and the Westerns. The level of proteins in the input was determined by measuring band intensity using the ImageJ program. Background was measured from a similar region on the gel and subtracted from each band. The ratio of Gem to Brm or Snr1 protein was then determined for each sample. To calculate the stoichiometry of interaction of Gem with Brm or Snr1, samples over-expressing Brm^{WT} or Snr1 were used. Since there was a background band at the size of Gem in the control pre-immune immunoprecipitation in the Snr1 experiment (Fig. 2B(i) lane 3), the amount of Gem protein in the Snr1 immunoprecipitation was adjusted by subtracting the band intensity of this background band. Calculations were made

using Microsoft Excel and Graphs were made using GraphPad Prism version 5.01.

Results

Drosophila Gem interacts genetically with members of the Brm complex

We have previously observed that Gem and Brm genetically interact in the *Drosophila* wing and eye (Seo et al., 2005). As Brm functions in a large protein complex (Dingwall et al., 1995; Papoulas et al., 1998), we sought to determine whether other Brm complex genes genetically interacted with Gem. We used the developing wing to examine this, since interactions were easier to score in this tissue relative to the eye. We expressed Gem (using the weaker *UAS-gem*^{43} transgene (Quinn et al., 2001) or Brm complex transgenes in wings via the *en-GAL4* driver, which is expressed in the posterior compartment of the developing wing. Expression of Gem produced adult flies with relatively normal wings (Fig. 1B and B') compared with wild-type flies (Fig. 1A and A'). Ectopic expression of Brm^{DN} led to a loss of the L5 wing vein and loss of the posterior cross vein (Fig. 1C and C'). Strikingly, ectopic expression of Brm^{DN} and Gem together using *en-GAL4* caused a dramatic developmental defect leading to lethality during the first instar larval stage (data not shown). This phenotype was much stronger than expected if Gem and Brm^{DN} effects were just additive, indicating that Gem and Brm^{DN} genetically interact.

We next tested a core member of the Brm complex, *snr1* for genetic interactions with *gem* in the wing using the *en-GAL4* driver. Expression of a dominant-negative form of Snr1, *Snr1-cdel.3* (Snr1^{DN}) (Zraly et al., 2003), gave a normal wing phenotype when expressed with *en-GAL4* (Fig. 1D and D'), but caused a shortening of wing vein L5 when co-expressed with Gem (Fig. 1E and E'). Thus, *gem* also genetically interacts in an antagonistic manner with snr during wing vein development.

To test whether Osa, a SWI1 homolog, and a component of the Brm–BAP complex also interacts with Gem, full-length wild-type *osa* (*UAS-osa*) (Collins et al., 1999), was expressed via the *en-GAL4* driver. Expression of *osa* resulted in a severe wing phenotype, including ectopic wing veins, blistering of the wing blade and reduced wing size (Fig. 1F and F'). We reasoned that if Gem acts antagonistically to the Brm–BAP complex, we would expect that the gain-of-function Osa phenotype would be suppressed by co-expression of Gem. Indeed *gem* expression strongly suppressed the *en-GAL4*, *UAS-osa* wing phenotype, although some blistering was still detectable (Fig. 1G and G'). This result showed that interactions between Gem and the Brm complex are not simply additive, but instead represent a functionally relevant interaction. Altogether this data shows that Gem interacts antagonistically with three components of the Brm–BAP complex (Brm, Snr1 and Osa) in the developing wing.

To validate these interactions in another tissue, we then examined effects of Gem and Brm complex genes on the embryonic peripheral nervous system (PNS), which we have previously shown to be affected by Gem over-expression to result in ectopic neurons (Quinn et al., 2001). Expression of Gem via the *en-GAL4* driver (expressed in the epithelial cells in the posterior compartment of each parasegment as well as PNS cells) or the *hairy-GAL4* driver (which is expressed in a similar domain to *en-GAL4* in the epidermis, but not in PNS cells), resulted in ectopic PNS cells as detected by 22C10 staining (Supp. Fig. 1), and reducing Brm complex function resulted in an enhancement of this effect (data not shown). However, upon closer examination it became

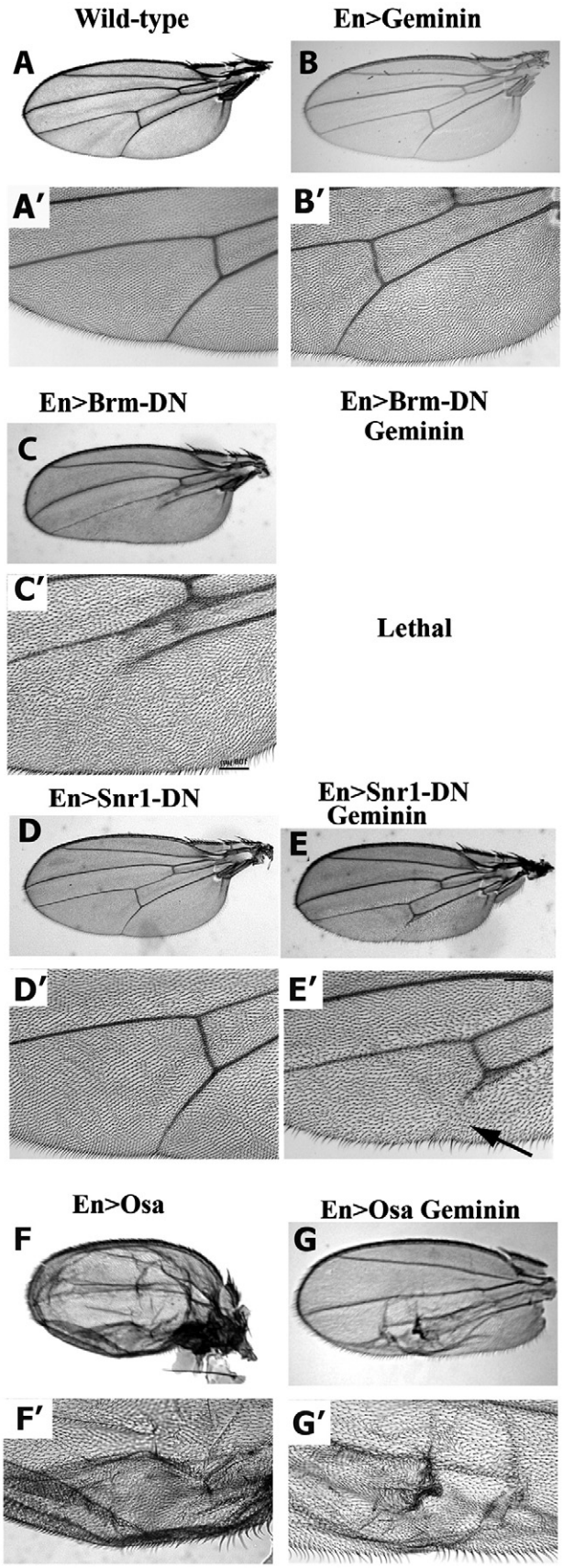

Fig. 1. Gem interacts antagonistically with other members of the Brm complex. Images of adult wings from *en-Gal4*, *UAS-GFP*/+ (Wild-type) (A), *UAS-gem*/*en-GAL4*, *UAS-GFP* (En>Gem) (B), *en-GAL4*, *UAS-GFP*/+; *UAS-brm*^{DN}/+ (En>Brm-DN) (C), *en-GAL4*, *UAS-GFP*/+; *UAS-snr1*^{DN}/+ (En>Snr1-DN) (D), *UAS-gem*/*en-GAL4*, *UAS-GFP; UAS-snr1*^{DN}/+ (En>Snr1-DN Gem) (E), *UAS-osa*/*en-GAL4*, *UAS-GFP* (En>Osa) raised at 18 °C (F) and *UAS-gem, UAS-osa*/*en-GAL4*, *UAS-GFP* (En>Osa Gem) raised at 18 °C (G). (A–G) 20× magnification, and (A'–G') 40× magnification of the posterior wing margin.

apparent that these ectopic neurons were not additional neurons, since there was also a loss of neural cells in the PNS, particularly in the lateral chordotonal neural clusters (lch5) (Supp Fig. 1). Thus, over-expression of Gem does not induce neural differentiation, as we originally reported (Quinn et al., 2001), but rather interferes with the normal position of the PNS neurons. The misplacement of the PNS neurons due to *gem* over-expression and the enhancement of this by brm^{DN} may be due to effects on the cell cycle, cell morphology or on signaling pathways affecting cell movement.

Gem and Brm physically interact in vivo

To test whether Gem and Brm complex proteins physically interact in *Drosophila*, we performed co-immunoprecipitation analysis with extracts from larval heads (which includes brains and eye, leg, haltere and wing imaginal discs) prepared from either wild-type larvae (*hsp70-GAL4* control), or larvae over-expressing the Brm^{WT} protein (see Materials and methods), the Brm complex protein, Snr1 (Zraly et al., 2003), or Gem under control of the *hsp70-GAL4* driver (see Materials and methods). When an anti-Gem antibody was used to immunoprecipitate Gem from *Drosophila*, a protein band that migrated at ~30 kDa, consistent with the molecular weight expected for Gem (Quinn et al., 2001), was detected (Fig. 2A lane 1, Fig. 2B lane 1). When anti-Brm antibody was used to immunoprecipitate Brm from wild-type extracts (hs-GAL4, Fig. 2A(i) lane 2) a ~30 kDa band was also detected with the anti-Gem antibody, although Brm itself was below detection levels in these extracts. This result shows that a complex forms between endogenous Gem and Brm proteins in *Drosophila* wing discs. The immunoprecipitation of Gem was specific, since this band was not detected in the control immunoprecipitations using pre-immune serum (Fig. 2A(i) lane 5). When Brm^{WT} protein was over-expressed in larval tissues, increased levels of Gem protein were observed in the immunoprecipitate (Fig. 2A(i) lane 3, quantified in 2A(iii)). Gem was also immunoprecipitated with Snr1 in wing discs over-expressing Snr1 (Fig. 2A(i) lane 4, Fig. 2B(i) lane 2). In this experiment, a protein ~30 kDa was detected in the control immunoprecipitation (Fig. 2B(i) lane 3), but at lower levels compared with that in the Snr1 immunoprecipitate (Fig. 2B(i) lane 2, quantified in Fig. 2B(iii)). Interestingly, in the reverse immunoprecipitation, with the Gem antibody from extracts over-expressing Gem, the Brm or Snr1 proteins were not detectable (Fig. 2A(i) lane 1, Fig. 2B(i) lane 1). This may be due to the relatively low level of Brm and Snr1 proteins present in the input and the detection of these proteins in the anti-Gem immunoprecipitates being beyond the sensitivity of the antibodies, or alternatively to the masking of Gem antibody epitopes by the interaction of Gem with Brm complex proteins. To determine the amount of Gem interacting with Brm and Snr1, we compared the % of Gem to Brm or Snr1 in the immunoprecipitations relative to the ratio of Gem to Brm or Snr1 in the input (Supp. Table 1). From the Brm^{WT} or Snr1 over-expression samples, we calculated that ~46% of total Gem immunoprecipitated with Brm and ~38% of total Gem was immunoprecipitated with Snr1 (see Materials and methods). Further analysis is needed to confirm this stoichiometry in the interaction of Brm and Snr1 proteins with Gem. Taken together, this data confirms and extends the results from the *Xenopus* system, showing that Brm, as well as another Brm complex component, Snr1, form complexes with Gem in *Drosophila* larval tissues.

Brm^{DN} does not enhance the effect of Gem on cell proliferation or survival in the developing wing

To determine the cellular basis for the interaction of Gem with compromised Brm function, we first explored whether these proteins may exert their effect by modulating cell proliferation. We have previously shown that over-expression of Gem inhibits DNA replication and leads to arrest in mitosis in the embryo (Quinn et al., 2001). We therefore examined whether expression of Brm^{DN} affects the cell cycle and whether co-expression of Brm^{DN} with Gem could enhance the effects of Gem on the cell cycle in wing discs. As shown in Fig. 3C, expression of the Gem^{43} transgene via the heat-shock inducible *hsp70-GAL4* driver resulted in a slight reduction of S-phase cells, as assayed by BrdU labeling in the wing disc compared with the control (Fig. 3A), while Brm^{DN} expression showed a slight increase in S-phase cells (Fig. 3B). However, when expressed with Gem, Brm^{DN} did not decrease the number of S-phase cells (Fig. 3B, M), as would have been expected if Brm^{DN} was enhancing the Gem phenotype through increasing the G1 to S-phase blockage. Gem expression also resulted in a slight increase in the number of mitotic figures, as revealed by phospho-Histone H3 (PH3) staining (Fig. 3G compared with 3E, and quantified in 3N), and in cell death, as assayed by TUNEL (Fig. 3K compared with 3I, and quantified in 3O) as expected based on previous findings (Quinn et al., 2001). Expression of Brm^{DN} alone had little effect on mitoses or cell survival (Fig. 3F, J). Importantly, co-expression of Brm^{DN} with Gem did not enhance these effects on mitosis or cell death (Fig. 3H, L and quantified in 3N, O), as would be expected if Brm^{DN} was acting with Gem on the cell cycle or cell death. Taken together, these results show that Brm^{DN} does not enhance the effect of Gem on cell proliferation or survival in the developing wing. Therefore, we conclude that this genetic interaction between Gem and Brm^{DN} must be occurring by another mechanism.

Gem and Brm^{DN} act antagonistically on EGFR–Ras–MAPK pathway signaling during wing development

Since expression of Gem in the background of compromised Brm function led to defects in wing vein development (Fig. 1), we sought to determine whether Brm and Gem might function to affect signaling pathways required for wing vein specification (De Celis, 2003; Guichard et al., 1999; Sotillos and De Celis, 2005). While the EGFR, Notch and Dpp signaling pathways are important for wing vein specification, we focused our attention on the EGFR signaling pathway in this study. The EGFR pathway plays important roles in many stages during *Drosophila* development (Baker and Yu, 2001; Tepass et al., 2002). During wing development of the *Drosophila* wing imaginal disc at the third instar larval stage, EGFR signaling is activated at the dorsal–ventral and anterior–posterior boundaries in the wing disc primordial (Brentrup et al., 2000; Crozatier et al., 2002). In *Drosophila*, the EGFR signaling pathway, acts through the Ras–MAPK signaling pathway to activate key target genes important for cell proliferation and wing vein formation (Karim and Rubin, 1998; O'Keefe et al., 2007a,b; Prober and Edgar, 2000).

To investigate whether EGFR–Ras–MAPK signaling was affected by brm^{DN} and *gem* expression, we examined their effect on these pathways in the wing imaginal disc. Since co-expression of brm^{DN} and *gem* via the *en-GAL4* driver was early larval lethal, we used *C96-GAL4* to drive expression of these genes. This driver is expressed in the dorsal–ventral boundary of the wing pouch, which gives rise to adult wing margin. The dorsal–ventral boundary of the larval wing disc coincides with the zone of non-proliferating cells (ZNC), where cells are arrested in either G1- or G2-phase (Johnston and Edgar, 1998). Therefore, using this driver provided the additional advantage of being able to examine the effects of Gem and Brm expression on the EGFR–Ras–MAPK signaling pathway in the wing disc independent of effects on the cell cycle. We have previously shown that *C96-GAL4*-induced expression of brm^{DN} and *gem* alone does not affect the adult wing, while co-expression of these genes leads to wing notching (Seo et al., 2005).

To monitor the effects of brm^{DN} and *gem* on the EGFR–Ras–MAPK pathway, we used an antibody to activated Erk/MAPK/Rolled (phospho-ERK, pERK). We also analyzed expression of the Notch pathway target, Cut, which is expressed in the dorsal–ventral boundary (Johnston and Edgar, 1998). The wild-type expression of

pErk and Cut was unaffected if either *gem* or brm^{DN} were expressed alone (Fig. 4B, C, F and G, compared with 4A and E), however, co-expression of brm^{DN} and *gem* caused a significant decrease in pERK staining (Fig. 4D), whilst Cut remained unaffected (Fig. 4H). This data shows that Gem and Brm^{DN} interfere with EGFR–Ras–MAPK pathway signaling, but do not affect expression of the Notch target, Cut, at the dorsal–ventral boundary during wing development.

To confirm these results, we investigated the reverse context by knocking down Gem and expressing wild-type Brm (Brm^{WT}). To reduce the levels of Gem, we generated transgenic flies containing a *UAS-gem* RNA interference (RNAi) construct, using the *pWiz* vector (Lee and Carthew, 2003; Narbonne-Reveau et al., 2008). In order to verify that the Gem-RNAi constructs were capable of knocking down Gem protein levels *in vivo*, we expressed *gem-RNAi* in third instar larval wing discs with *en-GAL4*. Ectopic expression of two independent insertions led to a clear reduction in Gem staining cells when compared with the anterior part of the wing disc (Supp. Fig. 2, and data not shown). To ectopically express Brm, we generated *UAS-*brm^{WT} transgenic flies, and showed that the transgene was expressed by Western analysis after heat-shock induction using the *hsp70-GAL4* driver (Supp. Fig. 3).

To determine whether *gem-RNAi* or brm^{WT} could up-regulate the Ras pathway signaling we used *en-GAL4* to express these genes in the posterior compartment of the wing disc, so that we could compare effects on pERK staining in the posterior compartment with that of the anterior compartment of the same wing disc. Expression of *gem-RNAi* via *en-GAL4* was mostly pupal lethal, alone as well as together with *brm* transgenes, while *en>*brm^{WT} alone or together with *gem* had no apparent effect on the adult wing phenotype (data not shown). In third instar larval wing discs, ectopic expression of *gem-RNAi* or brm^{WT} alone did not affect the levels of pERK staining relative to the anterior compartment or to wild-type (Fig. 5C and B, compared with A). However, co-expression of *gem-RNAi* with brm^{WT} resulted in a slight increase in pERK staining in the posterior compartment relative to the anterior compartment and compared with wild-type discs (Fig. 5D compared with A). We also analyzed the effect of expressing brm^{WT} together with *gem* in larval wing discs. Using the *en-GAL4* driver, expression of *gem* alone resulted in a slight decrease in pERK staining (Fig. 5E), however, expression of *gem* and brm^{WT} together restored pERK levels when compared with the anterior part of the disc or expression of *gem* alone (Fig. 5F, compare with E).

Interestingly, using the *en-GAL4* driver (in contrast to the apparently weaker *C96-GAL4* driver; Fig. 4) expression of brm^{DN} alone caused a dramatic reduction in pERK levels relative to the anterior compartment or to wild-type discs (Fig. 5G compared with A). This decrease in pERK levels by expression of Brm^{DN}, is consistent with the requirement of EGFR–Ras–MAPK signaling for wing vein formation and that reducing Brm function leads to a loss of wing veins (Fig. 1C). To examine the interaction of endogenous Gem with Brm^{DN} in this effect on pERK, we examined whether reducing Gem levels could suppress the reduction of pERK levels by Brm^{DN}. Indeed, expression of *gem-RNAi* and brm^{DN} together suppressed the decrease in pERK staining seen with brm^{DN} alone (Fig. 5H compared with G). Collectively, these results show that Gem and Brm act upon the EGFR–Ras–MAPK pathway in an antagonistic manner, with Brm promoting EGFR–Ras–MAPK signaling and Gem opposing this.

Gem and Brm genetically interact with a Raf (MAPKKK) gain-of-function phenotype in the wing

To further investigate the relationship between *gem* and *brm* and EGFR–Ras–MAPK signaling, we generated flies that expressed an activated allele of the MAPKKK/*Drosophila* Raf (Raf^{GOF} (Brand and Perrimon, 1994)), via the *C96-GAL4* driver in the dorsal–ventral compartment in the developing wing. *C96-GAL4*-driven expression of activated alleles of the EGF receptor result in wing notching and wing vein truncations (Settle et al., 2003), presumably due to aberrant differentiation or cell death. Similarly, we found that *C96-GAL4*-driven Raf^{GOF} resulted in wing notching and truncation of the veins (Fig. 6A (i)). When expressed alone via the *C96-GAL4*-driver *gem* or brm^{DN} had no significant effect on the adult wing phenotype, while co-expression of *gem* and brm^{DN} resulted in slight wing notching (Seo et al., 2005). Expression of *gem* or brm^{DN} alone in the *C96>*Raf^{GOF} background did not significantly affect the *C96>*Raf^{GOF} notched wing phenotype (Fig. 6A(ii, iv) compared with 6A(i)). However, halving the dosage of *brm* (using the brm^{2} null allele), showed a significant suppression of the *C96>*Raf^{GOF} notched wing phenotype (Fig. 6A(iii) and quantified in 6A(vii)). Importantly, co-expression of *gem* and brm^{DN}, or halving the dose of *brm*, in the *C96>*Raf^{GOF} background resulted in a significant suppression of the notched wing phenotype (Fig. 6A(v, vi) and quantified in 6A(vii)). Thus, although reducing Brm function alone can repress the effects of Raf^{GOF} on wing development, up-regulation of Gem together with compromised Brm function can more fully abrogate these effects.

We then tested whether decreasing Gem function could enhance the *C96>*Raf^{GOF} notched wing phenotype. Reducing the dosage of Gem, using two strong alleles, $gem^{k03202b}$ or gem^{k14019} in the *C96>*Raf^{GOF} background, caused a significant worsening of the Raf^{GOF} notched wing phenotype (Fig. 6B(ii–iii) compared with 6B(i), and quantified in 6B(iv)). Thus the Raf^{GOF} notched wing phenotype is sensitive to the levels of Gem. Taken together, these results show that when Raf–MAPK signaling is up-regulated the Gem and Brm levels can modulate the phenotypic effects of Raf^{GOF}. Furthermore, these data show that, consistent with the results described above, Gem and Brm act antagonistically on Raf–MAPK signaling.

Gem and Brm dominantly modify the rough eye phenotype due to expression of an activated allele of the EGFR in the eye

To explore whether Gem and Brm have physiological effects on the EGFR–Ras–MAPK signaling pathway more generally during *Drosophila* development, we examined their effects on EGFR signaling during eye development. To address this, we utilized a dominant activated allele of the EGFR, *ElpB1*, which produces a small and rough eye phenotype

Fig. 2. Gem and components of the Brm complex form a protein complex *in vivo*. (A) Gem, Brm and Snr1 interact in *vivo*. (i) Protein lysates from the heads of *hsp70-GAL4/+* (hs-Gal4), *hsp70-GAL4/+ ; UAS-*brm^{WT}*/+* (hs>brm^{WT}), *hsp70-GAL4/UAS-gem43* (hs>gem) and *hsp70-GAL4/+ ; UAS-Snr1/+* (hs>Snr1) heat-shocked (1 h heat shock, 1 h recovery) third instar larvae were immunoprecipitated with anti-Gem antibody (lane 1), anti-Brm antibody (lanes 2 and 3), anti-Snr1 antibody (lane 4) or rabbit pre-immune serum (lane 5, as a negative control) and immunoblotted with anti-Brm antibody (row 1) or anti-Gem antibody (row 2). All tracks are from the same gel, but intervening marker tracks have been removed. The Gem protein (~30 kDa) was detected when immunoprecipitated with Gem (lane 1), Brm (lane 2 and 3) or Snr1 (lane 4) antibodies. When over-expressed, the Brm protein (~180 kDa) was detected when immunoprecipitated with the Brm (lane 3) or Snr1 (lane 4) antibodies. (ii) Samples from the protein lysates, used for immunoprecipitations (30 μg compared with 330 μg), were run on a Western and immunoblotted with anti-Brm antibody (row 1), anti-Gem antibody (row 2) or anti-α-Tubulin antibody (row 3). Gem protein was more abundant when *gem* was over-expressed using the *hsp70-GAL4* driver, and Brm protein was higher when brm^{WT} was over-expressed using the *hsp70-GAL4* driver. (iii) Relative protein levels in the immunoprecipitations versus input (see Materials and methods). (B) Gem and Snr1 form a protein complex *in vivo*. (i) Protein lysates from the heads of *hsp70-GAL4/UAS-gem43* (hs>gem), *hsp70-GAL4/+ ; UAS-Snr1/+* (hs>Snr1) or *hsp70-GAL4/+* (hs-Gal4) heat-shocked (1 h heat shock, 1 h recovery) third instar larvae were immunoprecipitated with anti-Gem (lane 1), anti-Snr1 (lane 2) or rabbit pre-immune serum (lane 3, as a negative control) and immunoblotted with anti-Snr1 (row 1) or anti-Gem (row 2). All tracks are from the same gel, but intervening marker tracks have been removed. The Gem protein (~30 kDa) was detected when immunoprecipitated, Gem (lane 1) or Snr1 (lane 2) antibodies. The Snr1 protein was detected when immunoprecipitated with the Snr1 (lane 2) antibody. (ii) Samples from the protein lysates, used for the immunoprecipitations (20 μg compared with 220 μg), were immunoblotted with anti-Snr1 (row 1), anti-Gem (row 2) or anti-α-Tubulin (row 3). Snr1 protein was more abundant when *Snr1* was over-expressed using the *hsp70-GAL4* driver (note that, due to high levels of the Snr1 protein in this track, the band is whitened out), and Gem protein was higher when *gem* was over-expressed using the *hsp70-GAL4* driver. (iii) Relative protein levels in the immunoprecipitations versus input. In A(i, ii) and B (i, ii) +/– refers to ectopic expression of the protein.

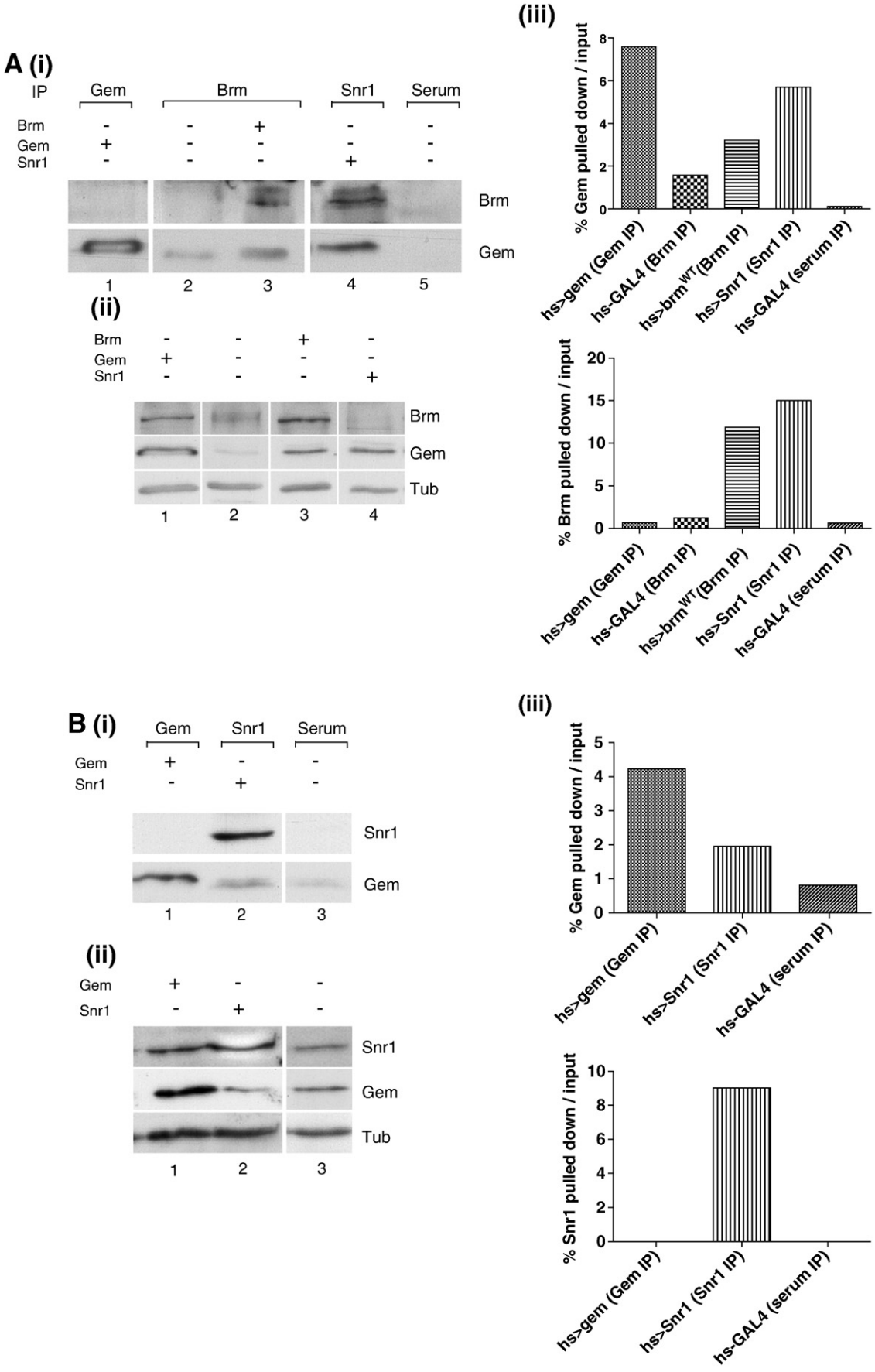
A (i)
IP
Gem
Brm
Snr1
Serum
Brm
Gem
Snr1
Brm
Gem
1 2 3 4 5
(ii)
Brm
Gem
Snr1
Brm
Gem
Tub
1 2 3 4
(iii)
% Gem pulled down / input
hs>gem (Gem IP)
hs-GAL4 (Brm IP)
hs>brm^WT(Brm IP)
hs>Snr1 (Snr1 IP)
hs-GAL4 (serum IP)
% Brm pulled down / input
B (i)
Gem
Snr1
Serum
Snr1
Gem
1 2 3
(ii)
Tub
(iii)
% Snr1 pulled down / input

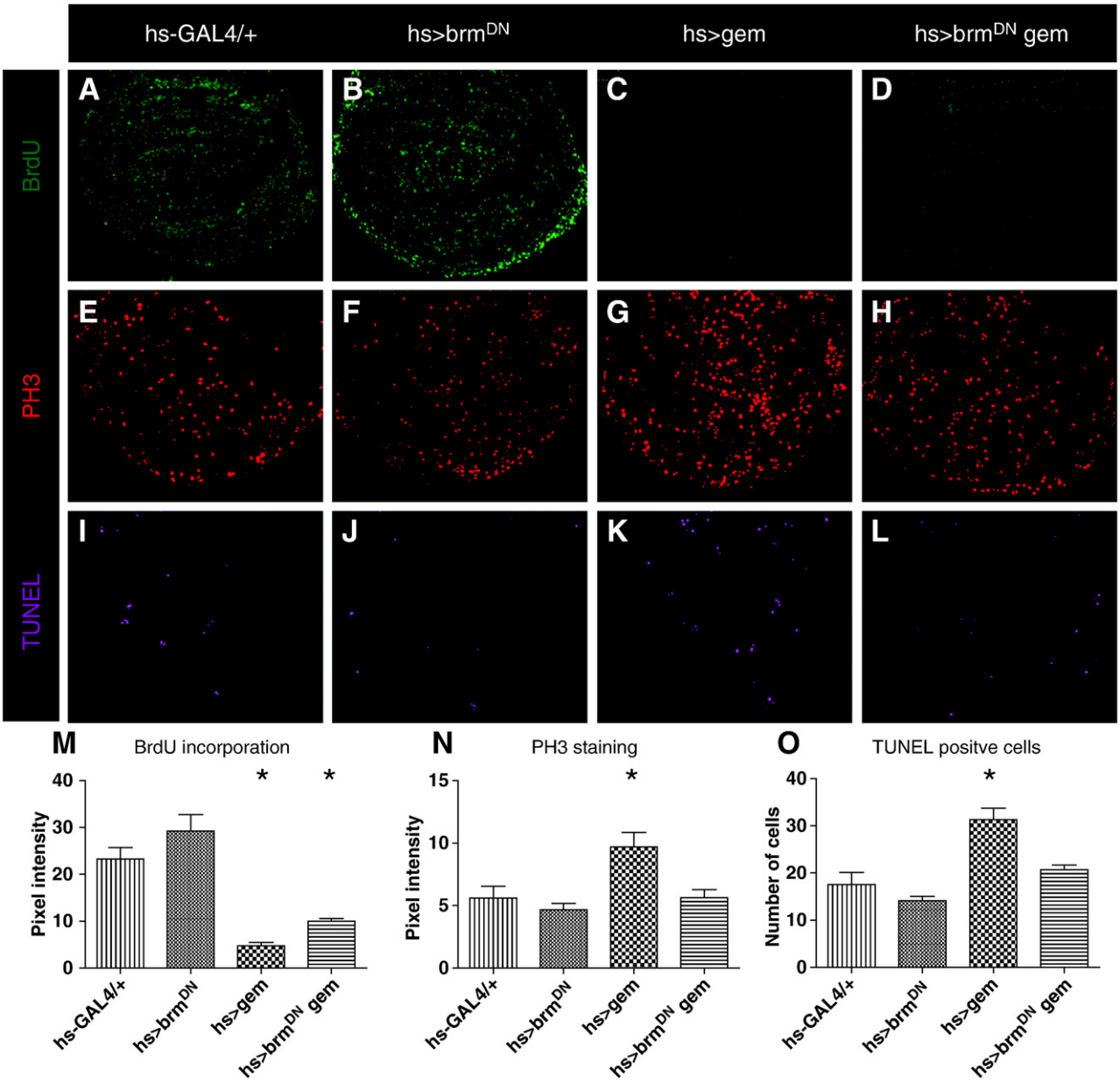

Fig. 3. The affect of Gem and Brm on the cell cycle and cell death. Confocal images of third instar larval wing imaginal discs which were heat shocked for 1 h and allowed to recover for 1 h of the following genotypes: *hsGAL4/+* (A, E, I); *hsGAL4/+; UAS-brm^{DN}/+* (hs>brm^{DN}) (B, F, J); *hsGAL4/UAS-gem* (hs>gem) (C, G, K); *hsGAL4/UAS-gem; UAS-brm^{DN}/+* (hs>gem brm^{DN}) (D, H, L). Discs were either labeled with BrdU (A, B, C, D), PH3 (E, F, G, H), or TUNEL (I, J, K, L). Over-expression of *gem* (hs>gem; C) or *gem* and a dominant-negative form of *brm* (hs>gem brm^{DN}; D) resulted in a significantly decreased amount of BrdU incorporation compared with wild-type (hsGAL4/+; A), as shown in a graph (M) representing the average pixel intensities of each genotype ($n>10$). The over-expression of *gem* (hs>gem) also resulted in significantly more PH3 staining (G) and TUNEL staining (K) compared with wild type-(hsGAL4/+) (E, I), also shown in graphs representing the average pixel intensities of each genotype for PH3 (N) or average number of TUNEL stained cells (O) ($n>10$). The *hs>gem* induced increase in PH3 and TUNEL staining was somewhat decreased by Brm^{DN} co-expression (H, L, N, O). Error bars = standard error of the mean. * = significantly different compared with the control using a One-Way ANOVA and Tukey test.

(Fig. 7B) compared with wild-type (Fig. 7A), primarily due to the decreased numbers of photoreceptor clusters formed (Baker and Rubin, 1989; Baker and Rubin, 1992; Baonza et al., 2001; Zak and Shilo, 1992). We expressed the Brm^{DN} genomic construct or reduced the dosage of *brm* or *gem* in the *EGFR^{ElpB1}* background. The small rough eye phenotype of *EGFR^{ElpB1}/+* was suppressed by expression of the *Brm^{DN}* gene (Fig. 7C) or by reducing the dose of *brm*, using the *brm^{2}* allele (Fig. 7D). Conversely, reducing the dose of *gem*, using the *gem^{k03203b}* allele enhanced the *EGFR^{ElpB1}/+* small rough eye phenotype (Fig. 7E). These results are consistent with the notion that reducing Brm activity can reduce EGFR–Ras–MAPK signaling, while reducing Gem activity can increase signaling through this pathway. Thus, the modulation of EGFR–Ras–MAPK signaling by Brm and Gem occurs similarly in the eye disc as it does in the wing disc (Figs. 4 and 5). The modulation of the *ElpB1* phenotype by Gem and Brm we observed occurs mostly by affecting the size of the eye, which can reflect changes in tissue growth, as well as differentiation. Since the *ElpB1* mutation affects photoreceptor cluster formation, cell proliferation and survival in the developing eye (Baker and Rubin, 1989; Baker and Rubin, 1992; Baonza et al., 2001; Zak and Shilo, 1992), further studies are required to determine the precise cellular effects of Brm and Gem on EGFR signaling in the eye.

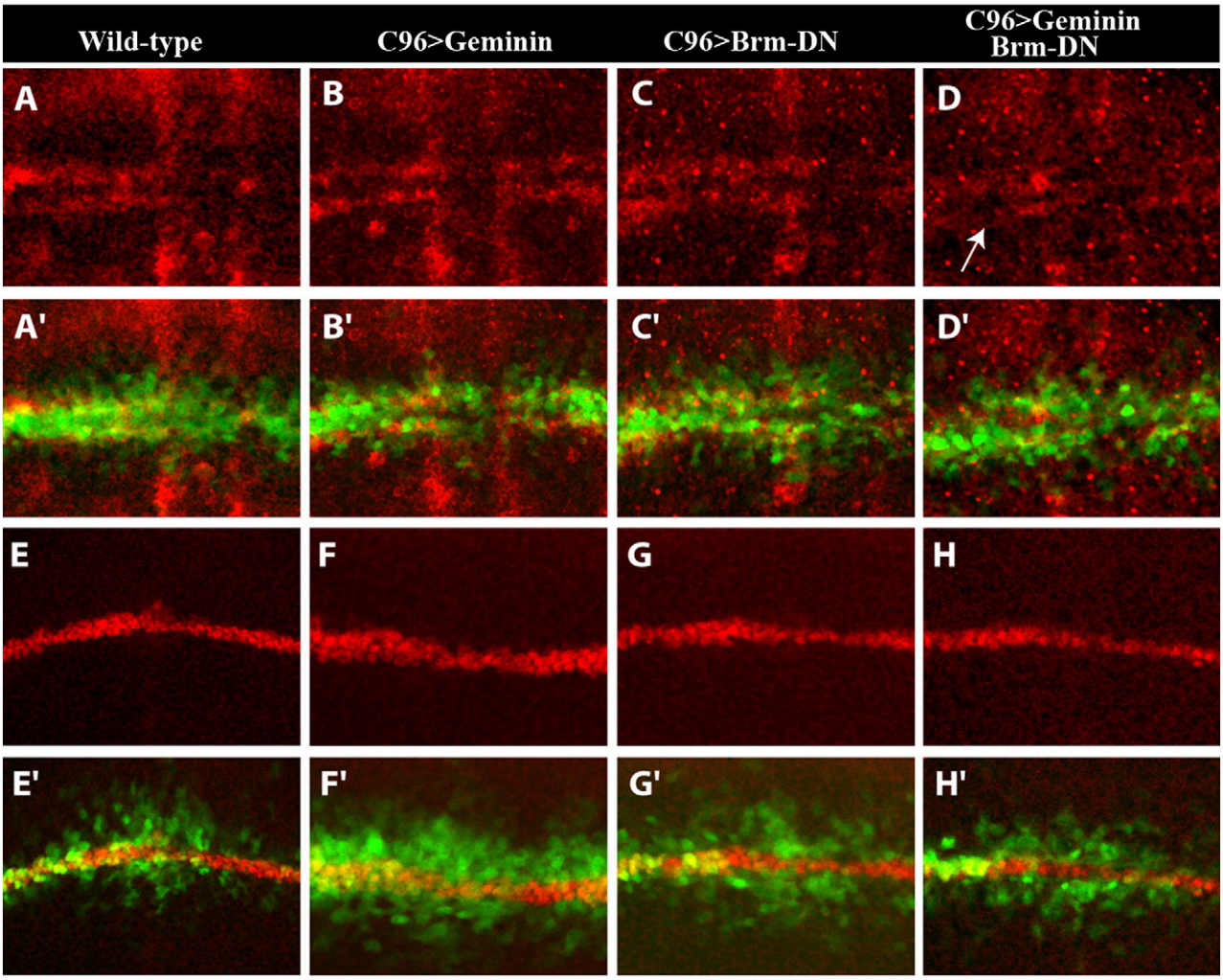

Fig. 4. Gem and Brm act antagonistically on the EGFR/Ras/MAPK pathway, but not the Notch pathway. Confocal images of third instar larval wing imaginal discs of the following genotypes *C96-GAL4*, *UAS-GFP*/+ (Wild-type) (A, A', E, E'), *UAS-gem*/+; *C96-GAL4*, *UAS-GFP* (C96>Gem) (B, B', F, F'), *UAS-brm^{DN}*/*C96-GAL4*, *UAS-GFP* (C96>Brm-DN) (C, C', G, G') or *UAS-gem*/+; *UAS-brm^{DN}*/*C96-GAL4*, *UAS-GFP* (C96>Gem Brm-DN) (D, D', H, H') were stained with antibodies to pERK/MAPK (A–D), or the Notch signaling pathway target, Cut (E–H). (A'–D') show a merge between pERK (red) and GFP (green) and (E'–H') show a merge between cut (red) and GFP (green). Note the reduction of pERK/MAPK staining upon *gem* and *brm^{DN}* co-expression (arrow in D).

Gem and Brm modulate pERK without affecting ERK levels

To further explore the effect of Gem and Brm on the EGFR–Ras–MAPK pathway, we assayed the effect of expressing Gem and Brm^{DN} by heat-shock induction using the *hsp70-GAL4* driver on pERK and total ERK levels in larval wing discs by Western analysis (Fig. 8A). In agreement with our immuno-fluorescence analysis, co-expression of Gem and Brm^{DN} reduced pERK levels (by ~50%), however ERK levels were similar to the control in all samples. Expression of Gem or Brm^{DN} alone did not result in decreased pERK or ERK levels (Fig. 8A). The amount of pERK slightly increased when *brm^{DN}* was over-expressed in this experiment although this was not consistent in other experiments (data not shown). Thus, in a background compromised for Brm function, expression of Gem alters ERK activation without affecting total ERK protein levels.

We also examined the effect of over-expression of wild-type Brm (Brm^{WT}) alone in *Drosophila* S2 (hemocyte-derived) tissue culture cells (see Materials and methods) or when expressed in wing discs via the *hsp70-GAL4* driver (Fig. 8B, C). In S2 cells, we found that Brm^{WT} expression resulted in an increase in pERK levels by 1.5 fold (Fig. 8B), without effects on ERK or Raf (MAPKKK) levels (Fig. 8B). Likewise, in wing disc samples over-expression of wild-type Brm alone increased pERK 1.45 fold (Fig. 8C). These results are consistent with the increased pERK levels observed when *brm^{WT}* and *gem-RNAi* were co-expressed via the *en-GAL4* driver (Fig. 5G).

Gem and Brm^{DN} cooperate to reduce MEK (MAPKK) levels

Next we sought to investigate the mechanism by which Brm^{DN} and Gem cooperate to decrease pERK levels. Using the same system of heat-shock induction of Brm^{DN}, Gem or both proteins in wing discs, described above, we analyzed the effect of these protein on activation of MEK (MAPKK/Sor), the kinase that phosphorylates and actives ERK (by using the pMEK antibody), and on total MEK levels. As shown in Fig. 9, while expression of Brm^{DN} or Gem alone resulted in slight decreases in MEK or pMEK levels, together they lead to a substantial reduction of both pMEK and MEK levels (to ~40% relative to the control). Thus, Brm^{DN} and Gem cooperate to decrease MEK protein levels, consistent with the reduced pERK levels observed (Figs. 4, 5 and 8).

Discussion

In this study, we have analyzed the interaction of *Drosophila* Gem with the Brm complex in cell proliferation, apoptosis and differentiation during development. We show that Brm and Snr1 can form a

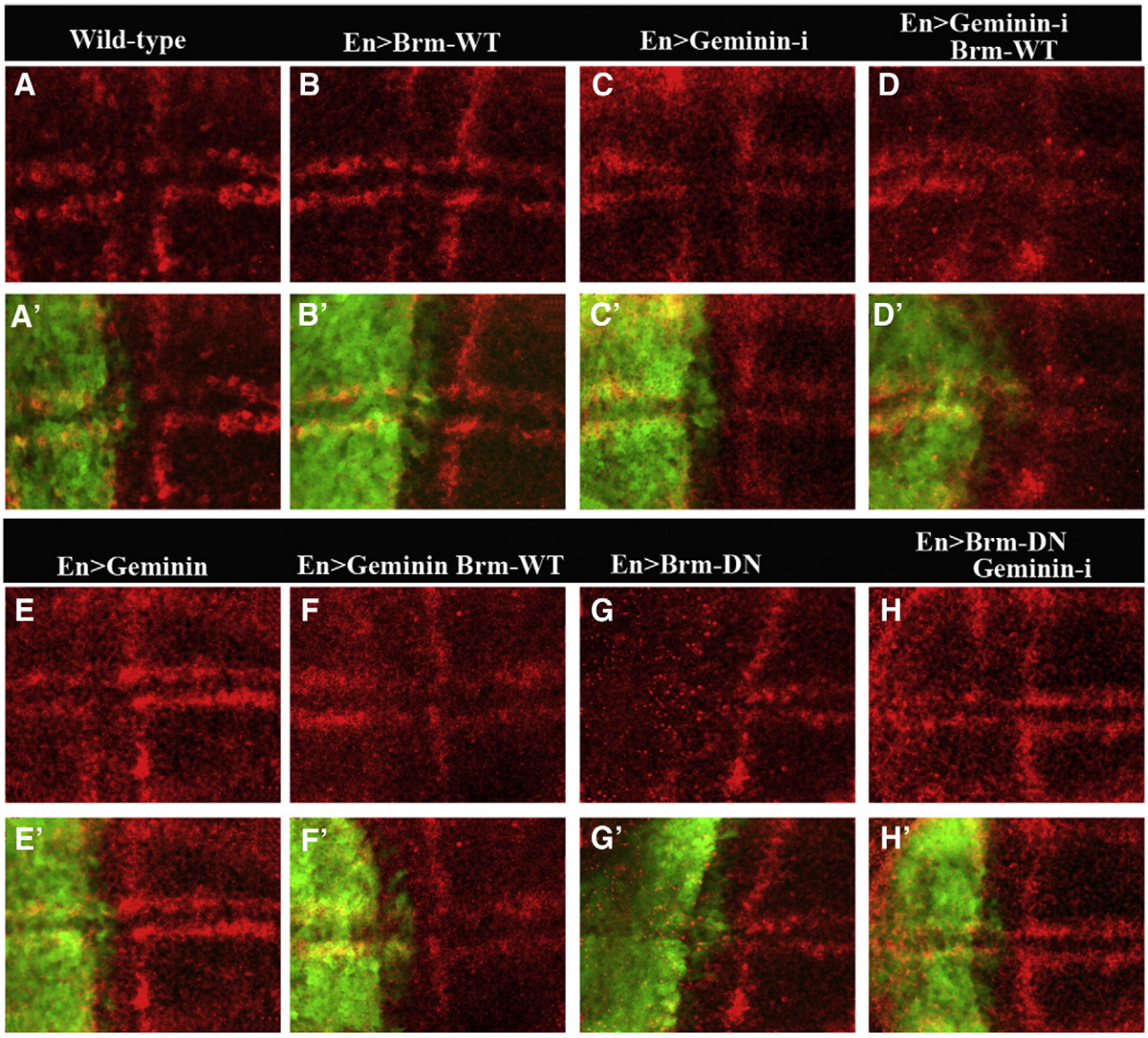

Fig. 5. Knockdown of Gem and over-expression of Brm^{WT} increases pERK levels. Confocal images of third instar larvae wing discs from *en-GAL4*, *UAS-GFP*/ + (Wild-type) (A, A'), *en-GAL4*, *UAS-GFP*/ +; *UAS-*brm^{WT}/ + (En>Brm-WT) (B, B'), *en-GAL4*, *UAS-GFP*/*UAS-dsRNA gem* (En>Gem-i) (C, C'), *en-GAL4*, *UAS-GFP*/*UAS-dsRNA gem*; *UAS-*brm^{WT}/ + (En>Gem-i Brm-WT) (D, D'), *en-GAL4*, *UAS-GFP*/*UAS-gem* (En>Gem) (E, E'), *en-GAL4*, *UAS-GFP*/*UAS-gem; UAS-*brm^{WT}/ + (En>Gem Brm-WT) (F, F'), *en-GAL4*, *UAS-GFP*/ +; *UAS-*brm^{DN}/ + (En>Brm-DN) (G, G') or *en-GAL4*, *UAS-GFP*/*UAS-dsRNA gem; UAS-*brm^{DN}/ + (En>Gem-i Brm-DN) (H, H'). Discs were stained with antibodies to pERK/MAPK in (A–H) and (A'–H') show a merge of pERK (red) and GFP (green).

complex with Gem in *Drosophila* larval tissue, and *gem* genetically interacts with *Brm*, *Snr1* and *osa*. Since Osa is the defining member of the Brm–BAP complex (Collins et al., 1999; Moshkin et al., 2007), these results implicate the Brm–BAP complex in the interaction with Gem. Our studies also revealed in three different ways that Brm acts antagonistically to Gem upon the EGFR–Ras–MAPK signaling pathway: firstly, reducing Brm function cooperates with Gem to decrease activation of ERK (pERK) in the developing wing disc; secondly, over-expressing Brm together with Gem knockdown results in increased pERK levels in the developing wing; and thirdly modulating Brm or Gem function modifies the wing and eye phenotypes of gain-of-function alleles in the EGFR–Ras–MAPK signaling pathway. Finally, we show that the mechanism by which Gem cooperates with compromised Brm function to decrease EGFR–Ras–MAPK signaling is by decreasing MEK (MAPKK) levels, consistent with the observed reduction in pERK levels.

The interaction of Gem with the Brahma complex

We have shown that Gem genetically interacts in an antagonistic manner with Brm and two other members of the Brm complex, Osa and Snr1 (Fig. 1). These interactions are consistent with a model where Gem inhibits, or is inhibited by Brm activity during wing development. The precise manner by which this interaction occurs is yet to be determined, however, our observation that Gem co-immunoprecipitates with Brm and Snr1 *in vivo* (Fig. 2), suggests that the antagonistic genetic interactions are likely to be mediated through physical association of Gem with the Brm complex. Further studies are required to determine whether the interaction between *Drosophila* Gem and Brm are direct, and whether Gem also physically interacts with other members of the Brm complex. Given our observation that Gem genetically interacts with Osa (Fig. 1), and Osa defines the Brm–BAP complex (Collins et al., 1999; Moshkin et al., 2007), it is likely that this

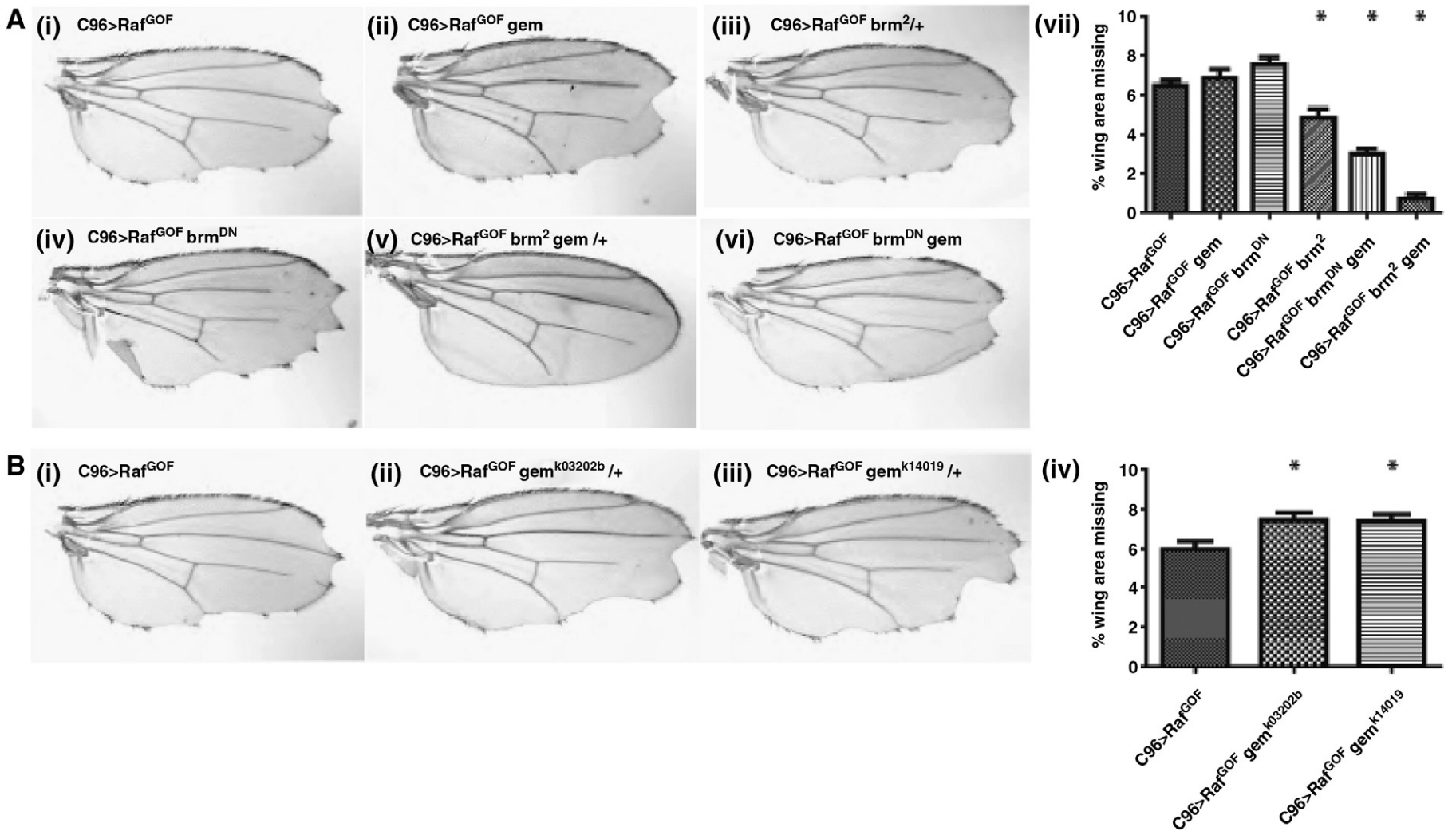

Fig. 6. Gem and Brm genetically interact with Raf^{GOF} in the wing. A Images of adult wings of the following genotypes: (i) *C96-GAL4*, *UAS-Raf^{GOF}*/+ (C96>Raf^{GOF}), (ii) *UAS-gem43*/+;*C96-GAL4*, *UAS-Raf^{GOF}*/+ (C96>Raf^{GOF} gem), (iii) *C96-GAL4*, *UAS-Raf^{GOF}*/*brm^{2}* (C96>Raf^{GOF} brm^{2}), (iv) *C96-GAL4*, *UAS-Raf^{GOF}*/*UAS-brm^{DN}* (C96>Raf^{GOF} brm^{DN}), (v) *UAS-gem43*/+;*C96-GAL4*, *UAS-Raf^{GOF}*/*brm^{2}* (C96>Raf^{GOF} gem brm^{2}), (vi) *UAS-gem43*/+;*C96-GAL4*, *UAS-Raf^{GOF}*/*UAS-brm^{DN}* (C96>Raf^{GOF} gem brm^{DN}). (vii) A graph representing the percentage of wing area missing due to the notching for each genotype. The percentage of wing area missing in C96>Raf^{GOF} (i) wings is significantly reduced when *gem* and *brm^{DN}* are co-expressed (vi) or upon halving the dose of *brm* (v). There was also a significant decrease in the C96>Raf^{GOF} wing area missing when halving the dosage of *brm* (iii). This was further suppressed when *gem* was also expressed (v). The suppression of the C96>Raf^{GOF} notching phenotype is also significant when comparing the over-expression of *gem* and *brm^{2}* together (v) versus *brm^{2}* alone (iii). B Images of adult wings of the following genotypes: (i) *C96-GAL4*, *UAS-Raf^{GOF}*/+ (C96>Raf^{GOF}), (ii) *gem^{k03202b}*/+; *C96-GAL4*, *UAS-Raf^{GOF}*/+ (C96>Raf^{GOF} gem^{k03202b}), (iii) *gem^{k14019}*/+; *C96-GAL4, UAS-Raf^{GOF}*/+ (C96>Raf^{GOF} gem^{k14019}). (iv) Quantification of wing tissue loss for each genotype (see Materials and methods). The percentage of wing area missing in C96>Raf^{GOF} (i) wings was significantly increased when the dosage of *gem* was decreased using the alleles, *gem^{k03202b}* (ii) or *gem^{k14019}* (iii). Error bars = standard error of the mean. * = significantly different compared with the control using a One-Way ANOVA and Tukey test.

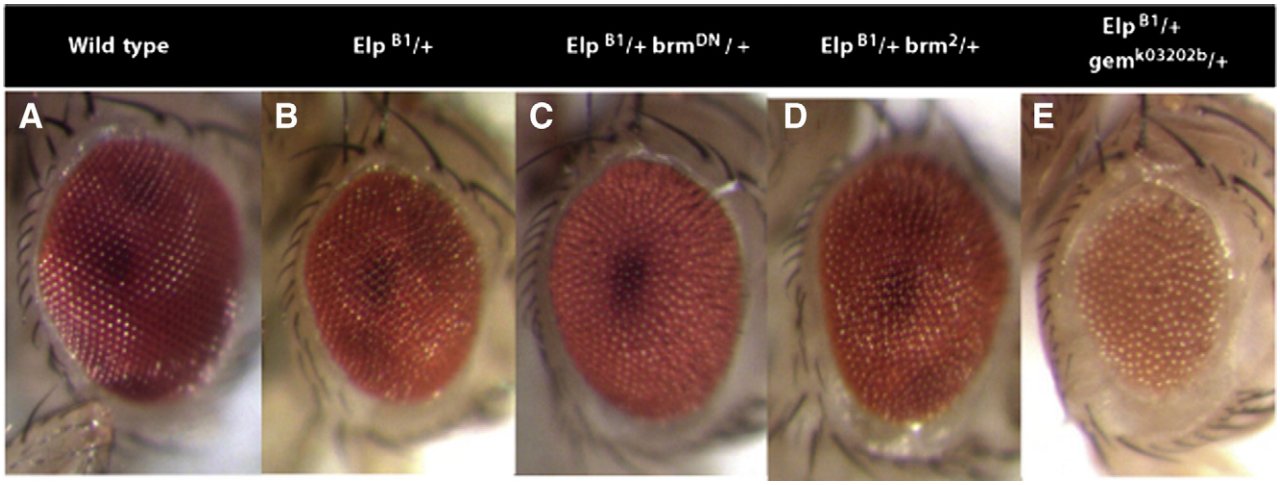

Fig. 7. Gem and Brm genetically interact with an activated allele of the EGFR in the eye. Images of male adult eyes of the following genotypes: (A) Canton-S (Wild Type), (B) $Elp^{B1}/+$, (C) $Elp^{B1}/+$; $brmDN/+$, (D) $Elp^{B1}/+$; $^{brm2}/+$, (E) $Elp^{B1}/+$; $gem^{k03202b}/+$.

complex physically interacts with Gem. However, additional analysis is needed to directly determine whether the defining components of the PBAP complex may also genetically and physically interact with Gem.

In *Xenopus*, Brg1 acts antagonistically with *Xenopus* Geminin and influences its neuralization function, which has been mapped to the N-terminal domain (Kroll et al., 1998; McGarry and Kirschner, 1998; Seo et al., 2005). However, in *Drosophila*, we have now shown that Gem does not induce neurogenesis in the developing embryo, but instead appears to result in a misplacement of peripheral nervous system cells (Supp. Fig. 1). In confirmation of this result, we have found that expression of the N-terminal domain of *Drosophila* Gem, which in *Xenopus* Geminin is capable of affecting neural differentiation (Kroll et al., 1998), has no affect on *Drosophila* embryonic or eye imaginal disc neural patterning (data not shown). By contrast, expression of a C-terminal fragment of *Drosophila* Gem, which mediates the DNA replication inhibitory function of Gem, also resulted in misplaced neural cells during embryogenesis (data not shown). This C-terminal fragment of *Drosophila* Gem also genetically interacts with Brm^{DN} (data not shown), however further experiments are necessary to determine if the binding between *Drosophila* Gem and Brm also requires acidic amino acids in the C-terminal tail, as occurs in *Xenopus* (Seo et al., 2005).

Regulation of EGFR–Ras–MAPK pathway signaling by the Brm complex and Gem

Surprisingly, we found that the enhancement of the phenotypic effects due to compromised Brm function by Gem over-expression, did not occur by Brm^{DN} enhancing Gem's effect on the cell cycle or cell death, but instead it is likely that Gem and Brm^{DN} interact by affecting differentiation of wing vein cell fate (Figs. 2 and 3). Indeed, we found that the EGFR–Ras–MAPK signaling pathway, important for wing vein specification (De Celis, 2003), was modulated by Brm and Gem. We found co-expression of *gem* and brm^{DN} inhibited EGFR–Ras–MAPK pathway signaling, as measured by phosphorylated Erk/MAPK/Rolled (pErk) staining (Fig. 4). Furthermore, expression of Brm^{DN} alone decreased EGFR–Ras–MAPK pathway signaling (Fig. 5G), whereas increasing Brm^{WT} expression promoted EGFR–Ras–MAPK pathway signaling (Fig. 8B, C). These results are consistent with the genetic interaction of the Ras pathway mutant, *vein*, with the Brm^{DN} eye phenotype observed in the study of Armstrong et al. (2005), which indicates that Brm^{DN} expression compromises EGFR–Ras–MAPK signaling. In addition, a recent study (Terriente-Felix and de Celis, 2009), has also shown that the Brm–BAP complex is linked to EGFR signaling. They showed that *osa* mutants were able to suppress Ras^{V12} or activated ERK (ERK^{SEM}) over-expression wing phenotypes. This genetic interaction is in agreement with our results that reducing Brm function alone was able to suppress phenotypes due to up-regulation of EGFR signaling (Figs. 6A (iii) and 7C, D). However, Terriente-Felix and de Celis (2009) found that in *osa* mutants pERK levels were variable, and therefore concluded that the Brm–BAP complex was required for sustained EGFR–Ras–MAPK signaling. They found that EGFR pathway targets, *rhomboid* (encoding a positive regulator of EGFR activity) and *argos* (encoding an inhibitory ligand of EGFR), were reduced in Osa-depleted cells, and therefore hypothesized that the Brm–BAP complex acts on the chromatin of these EGFR targets to modulate their expression. They argued that the effect of Osa depletion on the expression of these EGFR feedback targets and the opposing effects of Argos and Rhomboid on EGFR signaling, could explain the variable levels of pERK observed. In our analysis, the effect of Brm^{DN} expression via the *en-GAL4* driver on pERK was much more consistently reduced (Fig. 5G), than was observed by Terriente-Felix and de Celis (2009). It is possible that the variable effects that they observed may be due to a lower knock down of Brm–BAP complex activity in their system relative to ours. Indeed, in situations where Brm activity may not be knocked down as strongly in our experiments (i.e. when Brm^{DN} is expressed via the *C96-GAL4* or the *hsp70-GAL4* drivers), we did not observe a decrease in pERK levels (Fig. 4C and 8A). However, we observed that over-expression of Brm^{WT} (via the *en* or *hsp70* drivers) led to increased pERK levels (Fig. 5F and 8B, C). Although we have not looked at *rhomboid* or *argos* expression in our study, our results are compatible with their hypothesis that the Brm–BAP complex could act upon the chromatin of these and other EGFR targets to regulate the EGFR signaling pathway.

Our studies have shown that Gem and Brm affect pERK levels, and genetically interact with $EGFR^{Elp}$ and Raf/$MAPKKK^{GOF}$ phenotypes (Figs. 4–8), indicating that Gem and Brm act antagonistically on the EGFR–Ras–MAPK pathway. Moreover, we have shown that expression of Gem in a Brm compromised background resulted in decreased MEK levels, thereby explaining the decreased pERK in cells expressing Gem and Brm^{DN}. The precise mechanism by which Brm and Gem effect MEK levels will require further analysis, however, given the role of Brm in chromatin remodeling and transcriptional regulation of a large number of genes and the ability of Gem to interact with various transcription factors in other organisms, it is likely that the effect occurs at the level of MEK transcription. Whether up- or down-regulation of Brm can by itself affect MEK levels in situations where pERK levels are also affected will also require further investigation.

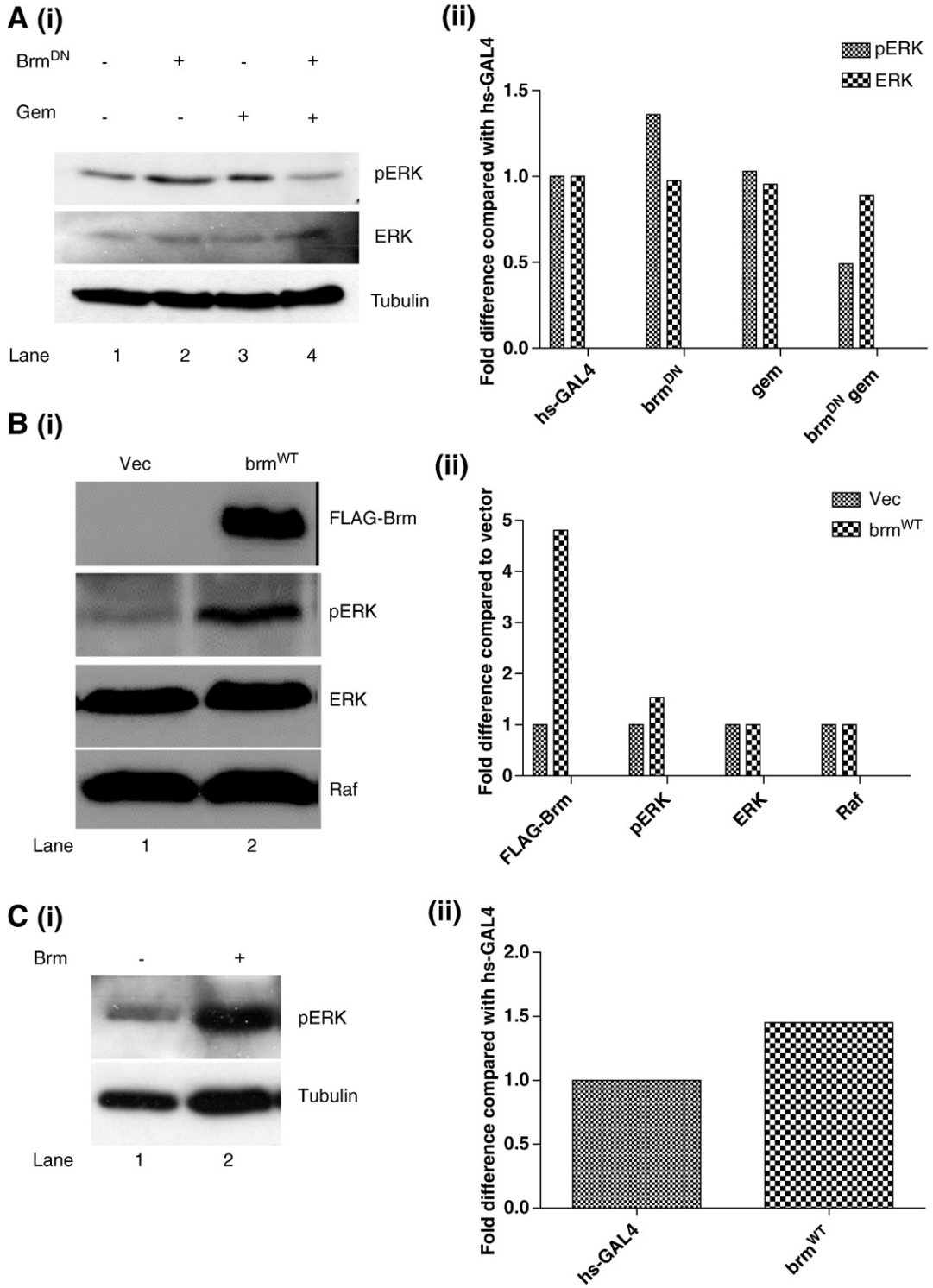

Fig. 8. Co-expression of Gem and Brm^{DN} reduces pERK activity. A (i) Protein lysates of wing discs of *hsp70-GAL4/+* (w^{1118}, lane 1), *hsp70-GAL4/+ ; UAS-brm^{DN}/+* (brm^{DN}, lane 2), *hsp70-GAL4/UAS-gem43* (gem, lane 3) and *hsp70-GAL4/UAS-gem43; UAS-brm^{DN}/+* (brm^{DN} gem, lane 4) heat shocked (1 h heat shock, 2 h recovery) third instar larvae were run on a Western and immunoblotted with phospho-ERK antibody (pERK, row 1), ERK antibody (ERK, row 2) and α-Tubulin antibody (Tubulin, row 3). The amount of pERK was similar when *brm^{DN}* or *gem* was over-expressed, but coexpression of *brm^{DN}* and *gem* resulted in a decrease in pERK levels. The amount of ERK was similar when either *brm^{DN}*, *gem* or both were over-expressed in the wing tissue. (ii) Quantification of band intensities (see Materials and methods). B (i) *Drosophila* S2 cells transfected with pMT/V5-His vector (Vec) or pMT/V5-His-FLAG-tagged brm (FLAG-brm) were incubated with 250 μM Cu^{2+}. Lysates were prepared and subjected to Western blotting with antibodies against FLAG to detect Brm (row 1), phospho-ERK (row 2), ERK (row 3) and Raf (row 4). Cells over-expressing ectopic *brm* increased the levels of activated phospho-ERK relative to vector control cells. The levels of ERK and Raf were similar between vector control and cells expressing ectopic *brm*. (ii) Quantification of band intensities. The levels of ERK and Raf were similar between control and cells over-expressing *brm*. C (i) Protein lysates of *hsp70-GAL4/+* (w^{1118}, lane 1) and *hsp70-GAL4/+; UAS-brm^{WT}/+* (brm^{WT}) heat shocked (1 h heat shock, 2 h recovery) third instar larvae heads were run on a Western and immunoblotted with phospho-ERK antibody (pERK, row 1) and α-Tubulin antibody (row 2). The amount of pERK increased when a wild-type *brm* was over-expressed compared with the control. (ii) Quantification of band intensities. In A(i) and C(i) +/– refers to ectopic expression of the protein.

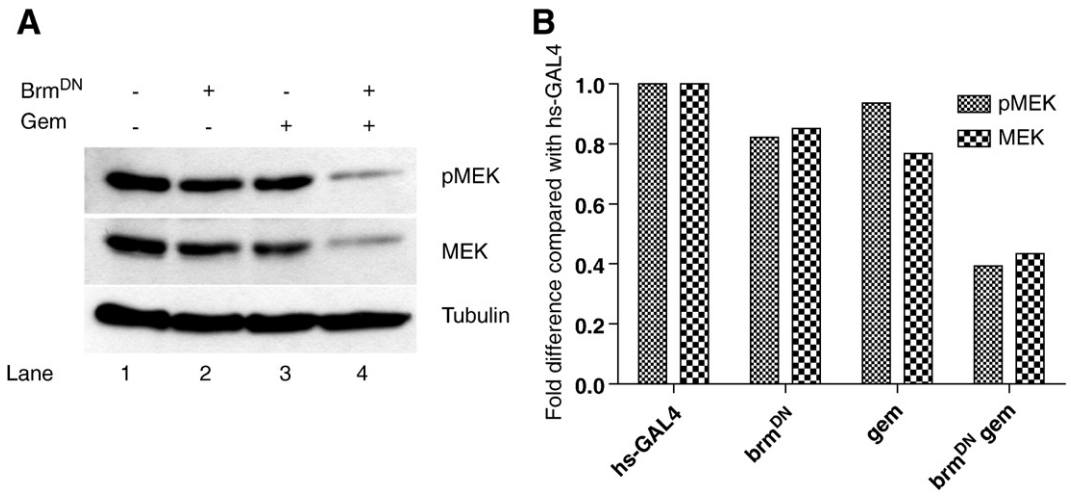

Fig. 9. (A) Gem and Brm^{DN} cooperate to reduce MEK levels. Protein lysates of wing discs of *hsp70-GAL4/+* (w^{1118}, lane 1), *hsp70-GAL4/+; UAS-brm^{DN}/+* (brm^{DN}, lane 2), *hsp70-GAL4/UAS-gem43* (gem, lane 3) and *hsp70-GAL4/UAS-gem43; UAS-brm^{DN}/+* (brm^{DN} gem, lane 4) heat shocked (1 h heat shock, 2 h recovery) third instar larvae were run on a Western and immunoblotted with phospho-MEK antibody (pMEK, row 1), MEK antibody (MEK, row 2) or α-Tubulin antibody (Tubulin, row 3). The levels of both MEK and pMEK were reduced when both *gem* and *brm^{DN}* (brm^{DN} gem) were co-expressed compared with the wild-type control (w^{1118}). The levels of pMEK and MEK protein were reduced when both *gem* and *brm^{DN}* were co-expressed (brm^{DN} gem) relative to the wild-type control (w^{1118}). (B) Quantification of band intensities (see Materials and methods) In A +/− refers to ectopic expression of the protein..

Since the EGFR signaling pathway is important for wing vein formation, the effects of Brm and Gem on the EGFR pathway are likely to explain the observed defects in wing vein formation. However, wing vein formation is also regulated by Notch and Dpp signaling (De Celis, 2003). We did not detect changes in Notch signaling in our experiments; modulating Gem and Brm activity had no effect on the expression of the Notch target, Cut, at the dorsal–ventral boundary of the developing wing (Fig. 4). However, the importance of the interaction of Gem and Brm in the modulation of the Dpp signaling pathway in wing vein specification remains to be determined. Since the Brm complex has been shown to interact with Dpp signaling in wing vein formation (Marenda et al., 2004), and Dpp signaling also affects the expression of the EGFR signaling regulator, Rhomboid (Yu et al., 1996), it is possible that Gem may also act to modulate Brm activity to control Dpp signaling in wing vein specification.

Possible role of Brm and Gem in EGFR–Ras–MAPK pathway regulation during development and in tumorigenesis

In *Drosophila*, the EGFR–Ras–MAPK signaling pathway is important for many aspects of differentiation during eye development (Baker and Rubin, 1989; Baker and Rubin, 1992; Baker and Yu, 2001; Baonza et al., 2001; Firth and Baker, 2005; Freeman, 1996; Zak and Shilo, 1992), and promotes vein cell fate specification in the developing wing (O'Keefe et al., 2007a,b). By contrast, hyperactivation of Ras signaling using a constitutively active allele (e.g. Ras^{V12}) leads to tissue overgrowth and cooperates with tumor suppressor mutants to form invasive tumors (Brumby and Richardson, 2005; Karim and Rubin, 1998). Therefore, maintaining the appropriate balance in EGFR–Ras–MAPK signaling activity in *Drosophila* is important for limiting cell proliferation and for cell fate decisions during development. Our results presented here, suggest that Gem and Brm may normally play a role in balancing EGFR–Ras–MAPK signaling activity during development, thereby affecting cell proliferation or differentiation.

In mammals, there is extensive evidence that the Ras–MAPK pathway is activated in tumorigenesis, making this pathway an important target for cancer therapy (Graham and Olson, 2007). However, high levels of flux through the Ras–MAPK signaling pathway can lead to cellular senescence and additional mutations are required to overcome this to allow tumor progression (Benanti and Galloway, 2004; Coleman et al., 2004; Han and Sun, 2007; McCormick, 1998; Nakagawa and Opitz, 2007; Yaswen and Campisi, 2007). Indeed, in human tumor cell lines, lower levels of oncogenic K-Ras expression appears to be favored (Konishi et al., 2007). Consequently, the level of oncogenic Ras expression is critical for whether it will play a role in cancer promotion or result in senescence. In mammalian cells, the Brm and Brg1 complexes inhibit cell cycle progression and are potential tumor suppressors (reviewed by Muchardt and Yaniv, 2001; Reisman et al., 2009). Despite its role as an inhibitor of DNA replication, Geminin is a candidate oncogene, as it is frequently over-expressed in several types of human tumors and is correlated with poor prognosis (reviewed by Montanari et al., 2006). Our observation that Brm acts to promote EGFR–Ras–MAPK signaling is seemingly at odds with Brm's role as a tumor suppressor. Likewise, our observation that Gem acts to block EGFR–Ras–MAPK signaling is opposite to its suspected oncogenic function. However, given the findings that very high levels of Ras signaling may promote senescence, the combined actions of decreased Brm function and Gem over-expression, which would be expected to result in decreased Ras signaling and prevent senescence, may indeed be tumor-promoting. Our results showing that Brm and Gem act in an opposing manner to regulate the EGFR–Ras–MAPK pathway, warrants further investigation of the involvement of Brm and Gem with the Ras signaling pathway during normal development and in tumorigenesis in *Drosophila*, mammalian cells and in human cancer.

Acknowledgments

We are grateful to Nick Dyson, Leonie Quinn, Tony Brumby, Michelle Longworth, Erica Sloan and Deborah Roczo for their advice during the course of this study and on the earlier versions of this manuscript, and to the three unknown reviewers for their insight and helpful comments. We particularly appreciate Nick Dyson's support in allowing some of the experiments in this study to be completed in his laboratory. We thank Peter Burke and Michelle Coombe for their technical help with the generation of transgenic flies. We thank Christian Muchardt for generously providing the Brm and Snr1 antibodies, John Tamkun for the *UAS-brm^{K804R}* flies, Richard Carthew for the *pWIZ* vector, Laura Johnston for the *en-GAL4*, *UAS-GFP* and *C96-GAL4* flies, Jessica Treisman for the *UAS-Osa* flies, Andrew Dingwall for the *UAS-Snr1* and *UAS-Snr1.cdel.3* flies, the Bloomington Center for providing other fly stocks and the Developmental Studies Hybridoma

Banks (DSHB) at the University of Iowa for antibodies. We also acknowledge the importance of the Flybase database for this study. This study was supported by grants from the Australian Research Council to H.E.R., to B.S. and H.E.R., and by the Peter MacCallum Cancer Center Special Purpose Funds. H.E.R. was supported by Welcome and NHMRC Senior Research Fellowships.

Appendix A. Supplementary data

Supplementary data associated with this article can be found, in the online version, at doi:10.1016/j.ydbio.2010.04.006.

References

Armstrong, J.A., Papoulas, O., Daubresse, G., Sperling, A.S., Lis, J.T., Scott, M.P., Tamkun, J. W., 2002. The Drosophila BRM complex facilitates global transcription by RNA polymerase II. Embo J. 21, 5245–5254.

Armstrong, J.A., Sperling, A.S., Deuring, R., Manning, L., Moseley, S.L., Papoulas, O., Piatek, C.I., Doe, C.Q., Tamkun, J.W., 2005. Genetic screens for enhancers of brahma reveal functional interactions between the BRM chromatin-remodeling complex and the delta-notch signal transduction pathway in Drosophila. Genetics 170, 1761–1774.

Baker, N.E., Rubin, G.M., 1989. Effect on eye development of dominant mutations in Drosophila homologue of the EGF receptor. Nature 340, 150–153.

Baker, N.E., Rubin, G.M., 1992. Ellipse mutations in the Drosophila homologue of the EGF receptor affect pattern formation, cell division, and cell death in eye imaginal discs. Dev. Biol. 150, 381–396.

Baker, N.E., Yu, S.Y., 2001. The EGF receptor defines domains of cell cycle progression and survival to regulate cell number in the developing Drosophila eye. Cell 104, 699–708.

Baonza, A., Casci, T., Freeman, M., 2001. A primary role for the epidermal growth factor receptor in ommatidial spacing in the Drosophila eye. Curr. Biol. 11, 396–404.

Bell, S.P., Dutta, A., 2002. DNA replication in eukaryotic cells. Annu. Rev. Biochem. 71, 333–374.

Benanti, J.A., Galloway, D.A., 2004. The normal response to RAS: senescence or transformation? Cell Cycle 3, 715–717.

Brand, A.H., Manoukian, A.S., Perrimon, N., 1994. Ectopic expression in Drosophila. Methods Cell Biol. 44, 635–654.

Brand, A.H., Perrimon, N., 1994. Raf acts downstream of the EGF receptor to determine dorsoventral polarity during Drosophila oogenesis. Genes Dev. 8, 629–639.

Brentrup, D., Lerch, H., Jackle, H., Noll, M., 2000. Regulation of Drosophila wing vein patterning: net encodes a bHLH protein repressing rhomboid and is repressed by rhomboid-dependent Egfr signalling. Development 127, 4729–4741.

Brumby, A.M., Richardson, H.E., 2005. Using Drosophila melanogaster to map human cancer pathways. Nat. Rev., Cancer 5, 626–639.

Brumby, A.M., Zraly, C.B., Horsfield, J.A., Secombe, J., Saint, R., Dingwall, A.K., Richardson, H., 2002. Drosophila cyclin E interacts with components of the Brahma complex. Embo J. 21, 3377–3389.

Bultman, S., Gebuhr, T., Yee, D., La Mantia, C., Nicholson, J., Gilliam, A., Randazzo, F., Metzger, D., Chambon, P., Crabtree, G., Magnuson, T., 2000. A Brg1 null mutation in the mouse reveals functional differences among mammalian SWI/SNF complexes. Mol. Cell 6, 1287–1295.

Coleman, M.L., Marshall, C.J., Olson, M.F., 2004. RAS and RHO GTPases in G1-phase cell-cycle regulation. Nat. Rev. Mol. Cell Biol. 5, 355–366.

Collins, R.T., Furukawa, T., Tanese, N., Treisman, J.E., 1999. Osa associates with the Brahma chromatin remodeling complex and promotes the activation of some target genes. Embo J. 18, 7029–7040.

Crozatier, M., Glise, B., Vincent, A., 2002. Connecting Hh, Dpp and EGF signalling in patterning of the Drosophila wing; the pivotal role of collier/knot in the AP organiser. Development 129, 4261–4269.

De Celis, J.F., 2003. Pattern formation in the Drosophila wing: the development of the veins. Bioessays 25, 443–451.

Del Bene, F., Tessmar-Raible, K., Wittbrodt, J., 2004. Direct interaction of geminin and Six3 in eye development. Nature 427, 745–749.

Diffley, J.F., 2004. Regulation of early events in chromosome replication. Curr. Biol. 14, R778–R786.

Dingwall, A.K., Beek, S.J., McCallum, C.M., Tamkun, J.W., Kalpana, G.V., Goff, S.P., Scott, M.P., 1995. The Drosophila snr1 and brm proteins are related to yeast SWI/SNF proteins and are components of a large protein complex. Mol. Biol. Cell 6, 777–791.

Elfring, L.K., Daniel, C., Papoulas, O., Deuring, R., Sarte, M., Moseley, S., Beek, S.J., Waldrip, W.R., Daubresse, G., DePace, A., Kennison, J.A., Tamkun, J.W., 1998. Genetic analysis of brahma: the Drosophila homolog of the yeast chromatin remodeling factor SWI2/SNF2. Genetics 148, 251–265.

Firth, L.C., Baker, N.E., 2005. Extracellular signals responsible for spatially regulated proliferation in the differentiating Drosophila eye. Dev. Cell 8, 541–551.

Freeman, M., 1996. Reiterative use of the EGF receptor triggers differentiation of all cell types in the Drosophila eye. Cell 87, 651–660.

Fujita, M., 1999. Cell cycle regulation of DNA replication initiation proteins in mammalian cells. Front Biosci. 4, D816–D823.

Graham, K., Olson, M.F., 2007. The ras signalling pathway as a target in cancer therapy. Recent Results Cancer Res. 172, 125–153.

Guichard, A., Biehs, B., Sturtevant, M.A., Wickline, L., Chacko, J., Howard, K., Bier, E., 1999. rhomboid and Star interact synergistically to promote EGFR/MAPK signaling during Drosophila wing vein development. Development 126, 2663–2676.

Han, J., Sun, P., 2007. The pathways to tumor suppression via route p38. Trends Biochem. Sci. 32, 364–371.

Hunter, T., Pines, J., 1994. Cyclins and cancer. II: Cyclin D and CDK inhibitors come of age. Cell 79, 573–582.

Johnston, L.A., Edgar, B.A., 1998. Wingless and Notch regulate cell-cycle arrest in the developing Drosophila wing. Nature 394, 82–84.

Karim, F.D., Rubin, G.M., 1998. Ectopic expression of activated Ras1 induces hyperplastic growth and increased cell death in Drosophila imaginal tissues. Development 125, 1–9.

Kingston, R.E., Bunker, C.A., Imbalzano, A.N., 1996. Repression and activation by multiprotein complexes that alter chromatin structure. Genes Dev. 10, 905–920.

Konishi, H., Karakas, B., Abukhdeir, A.M., Lauring, J., Gustin, J.P., Garay, J.P., Konishi, Y., Gallmeier, E., Bachman, K.E., Park, B.H., 2007. Knock-in of mutant K-ras in nontumorigenic human epithelial cells as a new model for studying K-ras mediated transformation. Cancer Res. 67, 8460–8467.

Kroll, K.L., Salic, A.N., Evans, L.M., Kirschner, M.W., 1998. Geminin, a neuralizing molecule that demarcates the future neural plate at the onset of gastrulation. Development 125, 3247–3258.

Lee, Y.S., Carthew, R.W., 2003. Making a better RNAi vector for Drosophila: use of intron spacers. Methods 30, 322–329.

Luo, L., Yang, X., Takihara, Y., Knoetgen, H., Kessel, M., 2004. The cell-cycle regulator geminin inhibits Hox function through direct and polycomb-mediated interactions. Nature 427, 749–753.

Lygerou, Z., Nurse, P., 2000. Cell cycle. License withheld—geminin blocks DNA replication. Science 290, 2271–2273.

Maiorano, D., Moreau, J., Mechali, M., 2000. XCDT1 is required for the assembly of pre-replicative complexes in Xenopus laevis. Nature 404, 622–625.

Marenda, D.R., Zraly, C.B., Dingwall, A.K., 2004. The Drosophila Brahma (SWI/SNF) chromatin remodeling complex exhibits cell-type specific activation and repression functions. Dev. Biol. 267, 279–293.

McCormick, F., 1998. Signal transduction. Why Ras needs Rho. Nature 394, 220–221.

McGarry, T.J., Kirschner, M.W., 1998. Geminin, an inhibitor of DNA replication, is degraded during mitosis. Cell 93, 1043–1053.

Mohrmann, L., Langenberg, K., Krijgsveld, J., Kal, A.J., Heck, A.J., Verrijzer, C.P., 2004. Differential targeting of two distinct SWI/SNF-related Drosophila chromatin-remodeling complexes. Mol. Cell. Biol. 24, 3077–3088.

Montanari, M., Macaluso, M., Cittadini, A., Giordano, A., 2006. Role of geminin: from normal control of DNA replication to cancer formation and progression? Cell Death Differ. 13, 1052–1056.

Moshkin, Y.M., Mohrmann, L., van Ijcken, W.F., Verrijzer, C.P., 2007. Functional differentiation of SWI/SNF remodelers in transcription and cell cycle control. Mol. Cell. Biol. 27, 651–661.

Muchardt, C., Yaniv, M., 2001. When the SWI/SNF complex remodels...the cell cycle. Oncogene 20, 3067–3075.

Nakagawa, H., Opitz, O.G., 2007. Inducing cellular senescence using defined genetic elements. Methods Mol. Biol. 371, 167–178.

Narbonne-Reveau, K., Senger, S., Pal, M., Herr, A., Richardson, H.E., Asano, M., Deak, P., Lilly, M.A., 2008. APC/CFzr/Cdh1 promotes cell cycle progression during the Drosophila endocycle. Development 135, 1451–1461.

Nishitani, H., Lygerou, Z., Nishimoto, T., Nurse, P., 2000. The Cdt1 protein is required to license DNA for replication in fission yeast. Nature 404, 625–628.

O'Keefe, D., Prober, D.A., Moyle, P.S., Rickoll, W.L., Edgar, B.A., 2007a. Egfr/Ras signaling regulates DE-cadherin/Shotgun localization to control vein morphogenesis in the Drosophila wing. Dev. Biol.

O'Keefe, D.D., Prober, D.A., Moyle, P.S., Rickoll, W.L., Edgar, B.A., 2007b. Egfr/Ras signaling regulates DE-cadherin/Shotgun localization to control vein morphogenesis in the Drosophila wing. Dev. Biol. 311, 25–39.

Papoulas, O., Beek, S.J., Moseley, S.L., McCallum, C.M., Sarte, M., Shearn, A., Tamkun, J.W., 1998. The Drosophila trithorax group proteins BRM, ASH1 and ASH2 are subunits of distinct protein complexes. Development 125, 3955–3966.

Prober, D.A., Edgar, B.A., 2000. Ras1 promotes cellular growth in the Drosophila wing. Cell 100, 435–446.

Quinn, L.M., Herr, A., McGarry, T.J., Richardson, H., 2001. The Drosophila Geminin homolog: roles for Geminin in limiting DNA replication, in anaphase and in neurogenesis. Genes Dev. 15, 2741–2754.

Reed, S.I., 1997. Control of the G1/S transition. Cancer Surv. 29, 7–23.

Reisman, D., Glaros, S., Thompson, E.A., 2009. The SWI/SNF complex and cancer. Oncogene 28, 1653–1668.

Reyes, J.C., Barra, J., Muchardt, C., Camus, A., Babinet, C., Yaniv, M., 1998. Altered control of cellular proliferation in the absence of mammalian brahma (SNF2alpha). Embo J. 17, 6979–6991.

Seo, S., Herr, A., Lim, J.W., Richardson, G.A., Richardson, H., Kroll, K.L., 2005. Geminin regulates neuronal differentiation by antagonizing Brg1 activity. Genes Dev. 19, 1723–1734.

Settle, M., Gordon, M.D., Nadella, M., Dankort, D., Muller, W., Jacobs, J.R., 2003. Genetic identification of effectors downstream of Neu (ErbB-2) autophosphorylation sites in a Drosophila model. Oncogene 22, 1916–1926.

Sotillos, S., De Celis, J.F., 2005. Interactions between the Notch, EGFR, and decapentaplegic signaling pathways regulate vein differentiation during Drosophila pupal wing development. Dev. Dyn. 232, 738–752.

Tepass, U., Godt, D., Winklbauer, R., 2002. Cell sorting in animal development: signalling and adhesive mechanisms in the formation of tissue boundaries. Curr. Opin. Genet. Dev. 12, 572–582.

Terriente-Felix, A., de Celis, J.F., 2009. Osa, a subunit of the BAP chromatin-remodelling complex, participates in the regulation of gene expression in response to EGFR signalling in the Drosophila wing. Dev. Biol. 329, 350–361.
Wohlschlegel, J.A., Dwyer, B.T., Dhar, S.K., Cvetic, C., Walter, J.C., Dutta, A., 2000. Inhibition of eukaryotic DNA replication by geminin binding to Cdt1. Science 290, 2309–2312.
Yaswen, P., Campisi, J., 2007. Oncogene-induced senescence pathways weave an intricate tapestry. Cell 128, 233–234.
Yu, K., Sturtevant, M.A., Biehs, B., Francois, V., Padgett, R.W., Blackman, R.K., Bier, E., 1996. The Drosophila decapentaplegic and short gastrulation genes function antagonistically during adult wing vein development. Development 122, 4033–4044.
Zak, N.B., Shilo, B.Z., 1992. Localization of DER and the pattern of cell divisions in wild-type and Ellipse eye imaginal discs. Dev. Biol. 149, 448–456.
Zraly, C.B., Marenda, D.R., Nanchal, R., Cavalli, G., Muchardt, C., Dingwall, A.K., 2003. SNR1 is an essential subunit in a subset of Drosophila brm complexes, targeting specific functions during development. Dev. Biol. 253, 291–308.